Int. J. Therm. Sci. (2000) 39, 141–172

S1290-0729(00)00236-2/REV

Review article

Stationary gas turbines and primary energies: A review of fuel influence on energy and combustion performances

Michel Molière *

General Electric Energy Products–Europe, 1 Avenue Charles Bohn, BP 379, 90007 Belfort, France

(Received 24 June 1999, accepted 21 September 1999)

Abstract — The gas turbine is a continuous-flow engine which develops steady aerodynamics and flame kinetics during stationary operation. These favourable features limit the constraints placed on fuel properties as to the performance of combustion and provide a considerable margin for devising clean combustion designs. This is why gas turbines have by essence access to a broad range of primary energies. However, due to the high specialisation of aero- and aeroderivative engines, this advantage is essentially exploitable by the Heavy Duty branch which, thanks to moderate compression ratios, robust mechanical designs and versatile combustion systems, can utilise a wide series of commercial and process by-products fuels: natural gas, petroleum distillates, *gasified coal* or *biomass, gas condensates, alcohols, ash-forming fuels* etc. In this context, a thorough knowledge of the multiple fuel/machine interdependences, which seem insufficiently covered by the existing literature on gas turbines, is of prime interest. This paper offers a consistent approach to three selected aspects of importance for gas turbine designers and users, which are: *energy conversion performances*; *combustion* and *emissions*. This approach includes: (i) a review of main primary energies accessible to stationary gas turbines, (ii) a new, differential method for assessing the influence of fuel on machine thermodynamics, with original equations accounting for performance changes versus fuel, (iii) a comprehensive discussion of how fuel properties impact on NO_x emission and combustion design. Finally, the main trends and prospects of gas turbine technology evolution, in terms of efficiency enhancement and low NO_x achievement, are tentatively outlined. © 2000 Éditions scientifiques et médicales Elsevier SAS

gas turbine / fuel / primary energy / thermodynamic performance / combustion / low NO_x / steam injection / water injection

Nomenclature

Roman symbols of variables

Cp_i^X	molar heat capacity of X at point i	$J{\cdot}K^{-1}{\cdot}mol^{-1}$
Cp_{ij}^X	average molar heat capacity of species X between points i and j	$J{\cdot}K^{-1}{\cdot}mol^{-1}$
$\check{C}p^X$	molar heat capacity of species X averaged between 288 and 2350	$J{\cdot}K^{-1}{\cdot}mol^{-1}$
e_{hf}	correction of GT efficiency for fuel enthalpy	
FAR	fuel–air ratio by mole $= n_f/n_a$	
H	specific enthalpy by mole	$J{\cdot}mol^{-1}$
Hex	heat flux at GT exhaust	W
Hin_{GT} or *Hin*	heat input into GT $= n_f LHV$	W
k_C	$= W_C/W_{GT}$	
k_T	$= W_T/W_{GT}$	
Lv	latent vaporisation heat by mole	$J{\cdot}mol^{-1}$
M	molecular mass	$kg{\cdot}mol^{-1}$
$LHV_{(T)}$	Low Heating Value of the fuel defined on a molar basis and at temperature T	$J{\cdot}mol^{-1}$
*LHV**	$= LHV_{(T)} - Cp_{28}^f(T_2 - T_8)$	$J{\cdot}mol^{-1}$
n	molar flow of a fluid	$mol{\cdot}s^{-1}$
P	pressure	Pa
q_f	change in mole number between air and combustion gas, referred to 1 mole of fuel (equation (40))	
R	8.314	$J{\cdot}mol^{-1}{\cdot}K^{-1}$
RI	diluent injection ratio $= n_d/n_f$	
SGF	specific combustion gas flow $= n_g/n_a$	
SHI	specific heat input into the gas cycle $= Hin/n_a$	$J{\cdot}mol^{-1}$
T	temperature	K
Tc	combustion temperature	K
Uc	flame speed	$m{\cdot}s^{-1}$
Vc	speed of burning gases	$m{\cdot}s^{-1}$
w	air humidity defined as the ratio (moles H_2O in air/moles of dry air)	
W	mechanical power	W

* Michel.Moliere@ps.ge.com

Greek symbols

$\alpha, \beta, \gamma,$		
δ, λ, μ	dimensionless cycle parameters as per equations (6a)–(6f)	
η	efficiency (polytropic data for turbine and compressor)	
π	compression ratio $= P_2/P_1 \approx P_3/P_4$	
φ	combustion richness or "equivalent ratio" $= FAR_{\text{actual}}/FAR_{\text{s}}$	
ν	molar N_2/O_2 ratio in air ≈ 3.76	
ρ	density	$\text{kg}\cdot\text{m}^{-3}$
τ	characteristic time	s
ω	stoichiometric coefficient of O_2 in the combustion of the fuel $C_cH_hO_oS_sN_n$	

Subscripts

1	air conditions at compressor inlet
2	compressor discharge
3	virtual conditions in combustors associated with the ISO firing temperature concept
$3'$	turbine rotor inlet (first stage rotating buckets)
$3''$	combustors outlet
4	turbine exhaust
5	exhaust of a CCGT (in flue gas stack)
8	fuel conditions at injection port
9	diluent conditions at injection port
a	air
b	combustion
$c, h, o,$	
s, n	stoichiometric coefficients in the fuel formula $C_cH_hO_oS_sN_n$
d	diluent (injected into the GT for $DeNO_x$ or power increase)
f	fuel
g	combustion gas
r	cooling of hot turbine parts
rz	(combustion) reaction zone
s	stoichiometric conditions
t	turbulent

Superscripts

0	"ISO conditions" of ambient air as per ISO 3977
a, f, g	(attached to *Cp*): see the same subscripts a, f, g

Abbreviations and acronyms

AI	auto-ignition
B	combustion system
BACT	best available control technology
C	compressor
CCGT	gas turbine combined cycle
CHP	combined heat and power (cogeneration)
FBN	Fuel Bound Nitrogen
GT	gas turbine
HCV	high calorific value fuel
HRB	Heat Recovery Boiler
IBC	ideal Brayton cycle
IGCC	integrated gasification combined cycle
IGV	compressor inlet guide vanes
INO_x	NO_x emission index of a fuel (base load emission figure referred to NG)
LCV	low calorific value fuel
LFL	Lower Flammability Limit
MCV	medium calorific value fuel
NG	natural gas
NGL	natural gas liquid
PAH	polyaromatic hydrocarbons
RQL	Rich-Quench-Lean combustion
SCR	selective catalytic reduction of NO_x (conversion of NO_x in N_2 by NH_3 on a catalyst)
SNG	substitute natural gas
T	expansion turbine
UFL	Upper Flammability Limit
UHC	unburnt hydrocarbons

1. INTRODUCTION

There is an increasing amount of literature being issued on gas turbines (GT) covering aspects as diverse as: *design* (turbomachinery; combustion, heat transfer); *performances*; *materials* (superalloys, coatings); *applications* (propulsion; power generation; mechanical drive; traction); *process control* etc.

However, gas turbine *fuels* are too often envisaged as mere heat sources for the gas cycle. Moreover, because middle-distillates overwhelmingly dominate the fuel pool of the aircraft industry, kerosene is often taken as the fuel paradigm in thermodynamic-oriented monographs and in combustion treatises. Papers devoted to stationary gas turbines and especially to power generation applications, usually mention natural gas and gasoil but they virtually ignore the numerous alternative fuels. Now *Heavy Duty gas turbines* are essentially fuel-flexible prime-movers. There is consequently an essential lack of literature addressing the wide sphere of fuels and the multiple interrelationships between gas turbine and fuel. Indeed, fuel impacts on most machine functions and systems, including: combustion; energy conversion performance; process control; selection of hot gas path materials etc. This many-facetted interdependence

is maximised in IGCC installations where the gas turbine exchanges *syngas*, *air* and *steam* with the gasification unit.

This paper aims to set out essential aspects of fuel/machine interactions in three selected, essential areas which are: *thermodynamic performance*, *combustion* and *gaseous emission*. In the author's opinion, a combined treatment of these three key-topics is worthwhile as it enables a "horizontal", multidisciplinary insight into GT technology, which can supplement more classic, "vertical" approaches available in specialised monographs.

2. THE TWO MAIN GAS TURBINE BRANCHES AND THEIR FUEL REPERTORIES

The numerous members of the present gas turbine family have two distinct origins: from the *industry* and from the *aviation*. This dual ascendance and the radical differences in applications have driven an early differentiation of both fuel repertories.

2.1. Aero- and aero-derived gas turbines

Aviation gas turbines or jet engines emerged during World War II. They have enjoyed since then an irresistible ascension both in the military and civil aircraft transport activities. Due to safety considerations and room restrictions for fuel storage, all aviation fuels are liquids. In fact, *kerosene* and civil/military *jet fuels* (Jet A1; JP4) following stringent formulations and quality control procedures are the exclusive fuels suitable for aircraft gas turbines.

The aeroderivative branch began to develop in the 60's as an extension of the jet engine activity. Manufacturers devised stationary packages of their aeroengines to take up earth-based niches, like mechanical drive and power generation, often in a competition with Diesel engines. Today, the most powerful aeroderivatives presently marketed are 40–50 MW-class engines which do not compete in size with the new large, 250 MW-class Heavy Duty products.

In addition to *kerosene* and *jet fuels*, aeroderivatives can burn *natural gas* and light, clean *gasoils*.

2.2. Heavy Duty gas turbines

The family of *Heavy Duty gas turbines* emerged during the 30's [1], which is much later than steam turbines. This historical shift is linked, besides high temperature material issues, to serious aerodynamics and manufacturing challenges posed by multistage air compressors along with the complex stall issues arising during start up and marginal operation. It is noteworthy that the function of air compression is replaced, in steam cycles, by the pumping of *liquid* feed water, a simpler, sooner mastered technology. Since the 60's, however, decisive strides achieved in manufacturing processes, aerodynamics, heat transfer, combustion and super-alloy science with valuable feed-backs from aircraft research programs have brought about huge progress in GT performance. In addition, Brayton cycles are exempt from a major drawback suffered by Rankine cycles which is the indirect heat transfer mode between the heat source and the working fluid: in steam cycles, heat exchange takes place through boiler tube walls. This limits hot source temperature and entails an irreversible exergy loss which can be alleviated in sophisticated cycles like the H_2O–NH_3 Kalina cycles [2], at the expenses, however, of simplicity and cost. In counterpart, the direct crossing of the expansion turbine by the combustion gas in gas turbines poses strict fuel purity requirements (ash or dust content).

The mid 80's were marked by the advent of *natural gas* as a major power generation energy [3] and the concurrent dissemination of two efficient GT based concepts: combined cycles (CCGT) and *cogeneration* or "Combined Heat and Power" (CHP). This enabled the mushrooming of GT based power plants presently experienced worldwide.

In comparison with aeroderivatives, Heavy Duty GT's feature: (i) higher power ranges but lower efficiency; (ii) larger installation footprint; (iii) simpler maintenance and, last but not least: (iv) a *wider fuel capability*.

Finally, in the quest for ever higher performances, Heavy Duty and aeroengines are experiencing parallel evolutions in many respects, including: firing temperature, metallurgy, combustion, turbine cooling devices, etc. [4].

2.3. The fuel panel of Heavy Duty gas turbines

Due to their robust designs and to less specialised combustion systems, Heavy Duty machines can handle a wide range of fuels [5, 6]. *Table I* shows a classification

TABLE I
Fuel panel of Heavy Duty gas turbines.

Industry branch	Origin process	Fuel name	State (L/G)	Characteristics range	Ashless (AL)/ ash forming (AF)
Oil	oil extraction	crude oil	L	light to heavy	AL
	oil distillation	LPG: propane, butane	L/G	variable C_3/C_4	
		naphtha, kerosene	L		AL
		gasoils	L	light to heavy	AL
		heavy oils	L	atm & vac residuals	AF
	catalytic cracking	Light/Heavy cycle oil	L	highly aromatic	AL
Natural gas (NG)	NG extraction	natural gas	G	– rich to weak – soft to sour	AL
	NG extr./treatment	gas condensates, NGL	L	light to heavy	AL to AF
	NG reforming	H_2	G	variable CO_2 content	AL
Coal lignite	coal extraction	coalbed gas	G	LCV gas	AL
	coal liquefaction	synfuels	L	highly aromatic	AL
		methanol	L	MCV liquid	AL
	coal gasification	syngas (CO/H_2), SNG	G	MCV to LCV	AL (purified)
Steel	coal pyrolysis	coke oven gas	G	MCV	AF
	iron production	blast furnace gas	G	LCV	AF
Petro-chemical industry	naphtha cracking	olefins	G	variable olefin %	AL
	aromatics synthesis	H_2-rich gas	G		AL
	butadiene unit etc.	C_3/C_4-rich gas	G		AL
Renewables and residuals	fermentation	biogas: CH_4–N_2–CO_2	G	MCV to LCV	AL (purified)
	gasification	syngas	G	MCV to LCV	AL (purified)

of most primary energies accessible to Heavy Duty GT's according to various criteria: (i) gas/liquid state; (ii) ashless/ash-forming and (iii) origin branch: *oil, gas, coal and renewable*.

3. FUELS AND THERMODYNAMIC PERFORMANCES

Maximising energy efficiency and minimising CO_2 emissions have become universal objectives. A consistent approach to the fuel-dependency of GT performances requires a short insight into turbomachine thermodynamics [7, 8].

The aim is not to cover the vast and complex issue of gas turbine performances, which requires sophisticated engineering softwares, but rather to produce a much simplified but comprehensive analysis of fuel effects in identifying the underlying fuel properties and the relevant equations. In this framework, an original, differential approach to fuel influence is proposed. *Mole-based properties* of fluids, though not customary in turbomachinery, are systematically used rather than mass-based properties, as the former are easier to handle when combustion reactions are involved.

In its simplest concept (single-shaft train; no compressor inter-cooler; nonregenerative cycle), a GT device comprises an air compressor C driven by an expansion turbine T, both turbomachines being connected through a combustion system B (*figure 1*). Some thermal energy (denoted Hin_{GT} or simply *Hin*, for *Thermal* or *Heat Input*) is injected into the combustors in the form of fossil fuel (formula: $C_cH_hN_nS_sO_o$). This heat input is defined as the product $n_f \cdot LHV$. It is noteworthy that *Hin* only accounts for the combustion heat of the fuel and *does not reflect the fuel temperature*. The raw shaft power is $W_{GT} = W_T - W_C$ and the GT efficiency is $\eta_{GT} = W_{GT}/Hin$. The sensible heat contained in the exhaust gases or *exhaust heat* is *Hex*. This data is essential when designing CCGT or CHP units as it represents the heat entering the Heat Recovery Boiler, or HRB (see Section 3.3.6).

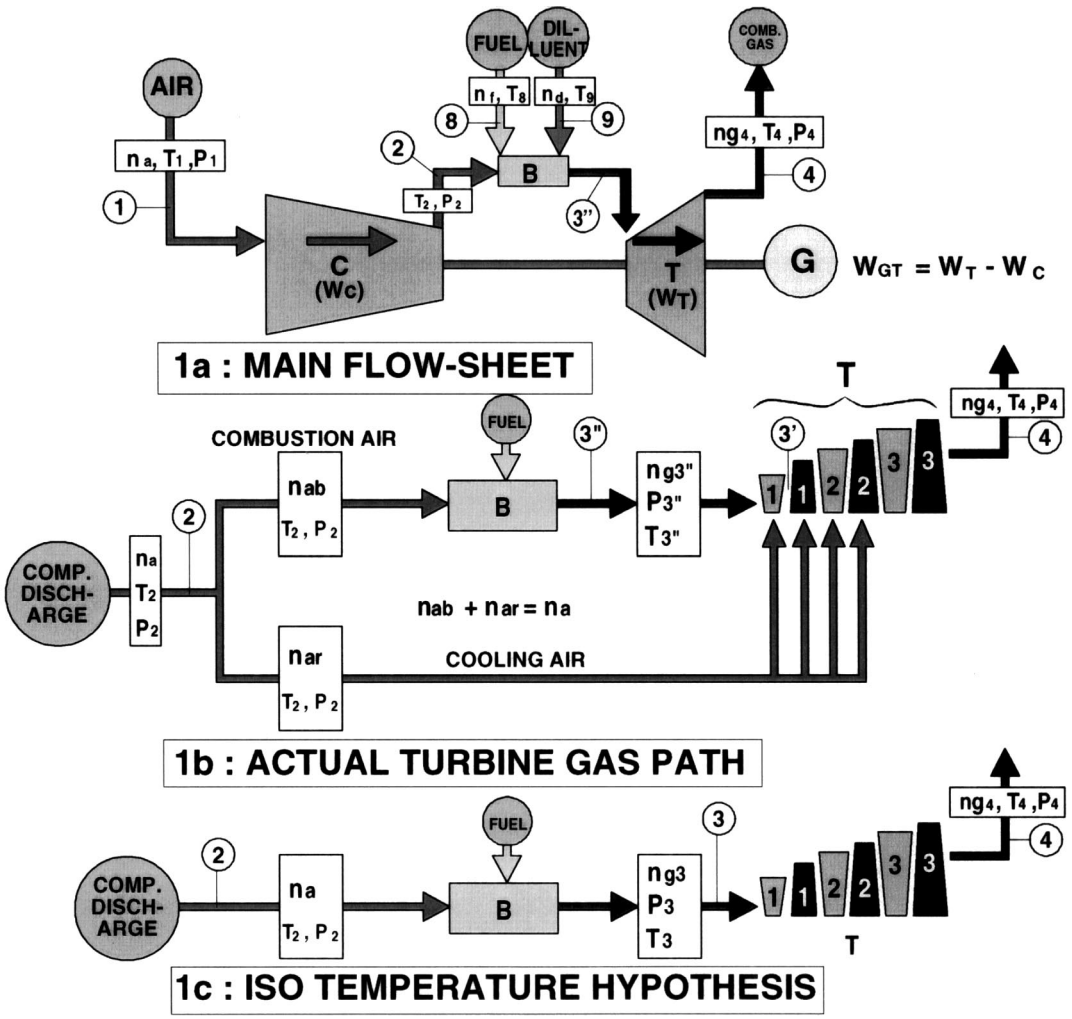

Figure 1. Gas turbine cycle schematics.

3.1. Differential approach to GT thermodynamics

A main difficulty faced when assessing W_{GT} and η_{GT} comes from the fact that W_{GT} is a difference between two greater terms: W_T and W_C, which both change with GT design, fuel and operation data. A second issue lies in the various air flows which are bled from the compressor and used to cool turbine hot parts. As shown in Appendix I, the notion of *ISO firing temperature* T_3 helps overcome this issue. A third delicate issue is the evaluation of the various energy losses.

In so far as one investigates the influence of fuel, a differential treatment enables to obviate these three issues as the corresponding effects are virtually fuel-independent and hardly affect cycle parameters, at least for fuels having usual *LHV* data (i.e. for MCV/HCV fuels). To this end, it is convenient to use *methane*, the most common fuel in stationary GT applications, as reference fuel and to introduce as basic parameters the ratios k_T and k_C be-

tween the power of the turbine (respectively of the compressor) and GT output (Appendix II):

$$W_T = k_T W_{GT} \quad \text{and}$$
$$W_C = k_C W_{GT} \quad (\text{which implies } k_T - k_C = 1) \tag{1}$$

The goal is to express each performance data (W, η, *Hex*) as a product of suitable physical factors so that a logarithmic differentiation will yield a sum of terms accounting each for a specific effect. To that end, one requires a set of base-variables. The choice made in this paper is for the 8 following cycle variables: n_g, T_1, T_3, η_C, η_T, Cp^g, π and e_{hf}.

This approach yields a first set of equations (see equations (34)–(36) in Appendix II).

In order to introduce fuel properties in these equations, one can use three further useful parameters (Appendix III):

– *FAR*: the *fuel–air ratio* is the fuel flow divided by the overall GT air flow: $FAR = n_f/n_a$ [mol·mol^{-1}],

– *SGF*: the *specific gas flow* is the combustion gas flow divided by the air flow: $SGF = n_{g3}/n_a$,

– q_f: the change, per fuel mole, in mole number between air and combustion gas: $q_f = (n_{g3} - n_a)/n_f = h/4 + o/2 + n/2$.

Appendix III shows that:

$$SGF \equiv \frac{n_{g3}}{n_a} = 1 + \frac{q_f n_f}{n_a} = 1 + q_f FAR = 1 + \left(q_f \frac{SHI}{LHV}\right) \tag{2}$$

where *SHI* is the *specific heat input* ($SHI = Hin/n_a$).

Since the last term of equation (2) (expression within brackets) is much smaller than 1, differentiating (2) yields:

$$\frac{dSGF}{SGF} = d\ln(SGF) \approx d(q_f FAR) \equiv d\left(q_f \frac{SHI}{LHV}\right) \tag{2'}$$

Introducing these parameters in equations (34)–(36) leads to a new set of equations which gives the change in performance entailed by slight variations of cycle conditions:

$$\frac{dW_{GT}}{W_{GT}} = k_T\, d(q_f FAR) - k_T \frac{dT_1}{T_1} + k_T \frac{dT_3}{T_3} + k_T(1-\beta)\frac{dCp^g_{34}}{Cp^g_{34}} + (k_T\beta - k_C\alpha)\frac{d\ln\pi}{\ln\pi} + k_C\alpha \frac{d\eta_C}{\eta_C} + k_T\beta \frac{d\eta_T}{\eta_T} \tag{3}$$

$$\frac{d\eta_{GT}}{\eta_{GT}} = k_C\, d(q_f FAR) - (k_C - \gamma)\frac{dT_1}{T_1} + (k_C - \gamma)\frac{dT_3}{T_3} + (k_C - k_T\beta)\frac{dCp^g_{34}}{Cp^g_{34}} + (k_T\beta - k_C\alpha + \alpha\delta)\frac{d\ln\pi}{\ln\pi} - de_{hf} + (k_C - \delta)\alpha\frac{d\eta_C}{\eta_C} + k_T\beta\frac{d\eta_T}{\eta_T} \tag{4}$$

$$\frac{dHex}{Hex} = d(q_f FAR) + \lambda\frac{dT_3}{T_3} - \lambda\frac{dT_1}{T_1} + (1+\mu)\frac{dCp^g_4}{Cp^g_4} - \mu\frac{d\ln\pi}{\ln\pi} - \mu\frac{d\eta_T}{\eta_T} \tag{5}$$

where:

– the 6 coefficients α, β, γ, δ, λ and μ depend only on the 4 cycle temperatures ($T_1, \ldots, T_4$):

$$\alpha = T_2 \frac{\ln(T_2/T_1)}{T_2 - T_1} \tag{6a}$$
$$\beta = T_4 \frac{\ln(T_3/T_4)}{T_3 - T_4} \tag{6b}$$
$$\gamma = \frac{T_2}{T_3 - T_2} \tag{6c}$$
$$\delta = \frac{T_2 - T_1}{T_3 - T_2} \tag{6d}$$
$$\lambda = \frac{T_4}{T_4 - T_1} \tag{6e}$$
$$\mu = T_4 \frac{\ln(T_3/T_4)}{T_4 - T_1} \tag{6f}$$

– the term e_{hf} is the fraction of the energy input (*Hin*) spent to heat the fuel from its supply temperature T_8 (8 being the label of the fuel injection point) to the compressor discharge temperature T_2. e_{hf} is given by the following formula:

$$e_{hf} = \frac{Cp^f_{28}(T_2 - T_8)}{LHV} \tag{7}$$

This corrective term is not always minute and must not be omitted in the expression of the GT efficiency (equation (4)).

One must note that a further development of $d(q_f FAR)$ in equations (3)–(5) is not possible as q_f may undergo not infinitely small but discrete changes when changing fuel.

To use these equations, one needs expressions of *FAR*, Cp^g, π, η_C, η_T and their differentials. It is easy to show that

$$FAR \approx \frac{Cp_{23}^{a}(T_3 - T_2)}{LHV^*}\left[1 + \frac{\Delta_{Cp} Cp_{23}^{a}(T_3 - T_2)}{LHV^*}\right]$$

where

$$\Delta_{Cp} = \frac{c Cp_{23}^{CO_2} + \frac{h}{2} Cp_{23}^{H_2O} + s Cp_{23}^{SO_2} + \frac{n}{2} Cp_{23}^{N_2} - \omega Cp_{23}^{O_2}}{Cp_{23}^{a}}$$

The difference $\Delta(q_f FAR)$ between two fuels can be deduced from both equations. Cp_{23}^{g} can be written:

$$Cp_{23}^{g} \approx Cp_{23}^{a}\left\{1 + \frac{[\Delta_{Cp} - q_f Cp_{23}^{a}](T_3 - T_2)}{LHV^*}\right\}$$

Now, according to Note 5, a good estimate of dCp_{34}^{g}/Cp_{34}^{g} is dCp_{23}^{g}/Cp_{23}^{g}, which leads to

$$\frac{dCp_{34}^{g}}{Cp_{34}^{g}} \approx (T_3 - T_2) Cp_{23}^{a}\, d\left[\frac{\Delta_{Cp} - q_f}{LHV^*}\right]$$

From equations (8) and (8′), one draws:

$$\pi \approx K n_{g3} M_{g3}^{1/2} T_{3'}^{1/2} \left(Cp_3^{g}\right)^{0.107}$$

and

$$\frac{d\pi}{\pi} = \frac{dn_{g3}}{n_{g3}} + 0.5\frac{dM_{g3}}{M_{g3}} + 0.5\frac{dT_3}{T_3} + 0.107\frac{dCp_3^{g}}{Cp_3^{g}}$$

with

$$M_g = M_a \frac{1 + [\Delta_M FAR]}{1 + q_f FAR} \approx M_a\left[1 - (q_f - \Delta_M)FAR\right]$$
$$= M_a(1 - \varepsilon_M)$$

where

$$\Delta_M = \frac{c M_{O_2} + \frac{h}{2} M_{H_2O} + s M_{SO_2} + \frac{n}{2} M_{N_2} - \omega M_{O_2}}{M_a}$$

and

$$\frac{dM_g}{M_g} \approx d\left[(q_f - \Delta_M)FAR\right]$$

The access to η_C, η_T needs the knowledge of compressor and turbine characteristics. In practice, however, $d\eta_C$ and $d\eta_T$ are small when changing fuel (see Section 3.2.3).

3.2. Quantifying the influence of fuel

A glance at equations (3)–(5) shows the fuel properties which influence GT performances: (i) the term ($q_f FAR$), an image of the combustion gas flow; (ii) the compression ratio π; (iii) the heat capacity of combustion gas, Cp^g; (iv) turbine efficiency η_T; (v) e_{hf}, an image of fuel temperature and, indirectly: (vi) compressor efficiency η_C (through π).

The outcomes of equations (3)–(5) can be illustrated in considering, for instance, a typical "second generation" Heavy Duty GT burning methane in ISO conditions ($T_1 = 288$ K, $P_1 = 1.013$ bar) and operating at "base load". "*Base load*" operation means that the firing temperature T_3 equals the full design value and *ideally* does not change from one fuel to another.

Base load parameters are: $n_a = 4\,948$ mol·s^{-1}; $n_g = 5\,104$ mol·s^{-1}; $FAR_{CH_4} = 0.031$; $T_2 \approx 622$ K, $T_3 \approx 1\,325$ K, $T_4 \approx 805$ K, $\pi \approx 12.05$, $k_T \approx 2.162$. *Table II* gives the corresponding values of the coefficients contained in formulae (3)–(5).

Table III illustrates the impacts of 8 fuels on the performance data (W_{GT}, η_{GT} and *Hex*) of the same GT model running also at base load. Methane is taken as reference fuel. The coefficient c in formula $C_cH_hN_nS_sO_o$ has been normalised and taken equal to 1 (except of course for H_2). In fact, actual temperature control curves do not keep T_3 rigorously constant at base load, but this does not affect the ranking of fuels. *Table III* also gives the NO_x emissions, expressed in ppm VW, or parts par million by volume on a wet basis (a dry basis would penalise H_2 which only produces H_2O).

3.2.1. Influence of the fuel on the combustion gas flow (parameter $q_f FAR$)

Equations (3) and (4) show that a higher ($q_f FAR$) data, entailing a higher flow of combustion gas (n_{g3}: equation (2)), tends to improve performances. In particular, the following composition changes have positive effects on W_{GT} and η_{GT}:

TABLE II
Matrix of coefficients contained in equations (3)–(5) ($T_3 \approx 1050$ °C, $\pi \approx 12$). Fuel: methane.

	dT_1/T_1	dT_3/T_3	$d(q_f FAR)$	$d\eta_C/\eta_C$	$d\eta_T/\eta_T$	dCp^g/Cp^g	$d\ln\pi/\ln\pi$	de_{hf}
dW_{GT}/W_{GT}	−2.162	2.162	2.162	2.325	2.015	0.495	$6 \cdot 10^{-3}$	0
$d\eta_{GT}/\eta_{GT}$	−0.278	0.278	1.162	0.987	1.667	−0.507	0.680	−1
$dHex/Hex$	−1.557	1.557	1	0	−0.776	1.776	−0.776	0

TABLE III
Influence of various fuels on power output and efficiency (same GT as in *table II*). Operation conditions: base load ($T_3 = \text{const}$); ambient conditions: 15 °C, 1 atm, air humidity: 0 %.

Fuels	Molecular formula[1] $C_cH_hO_oS_sN_n$	$LHV_{(15°C)}$ [kJ·mol^{-1}]	$LHV_{(T_2)}$[2] [kJ·mol^{-1}]	q_f ($= h/4 + n/2 + o/2$)	$\frac{dW_{GT}}{W_{GT}}$ [%]	$\frac{d\eta_{GT}}{\eta_{GT}}$ [%]	$\frac{dHex}{Hex}$ [%]	NO_x [ppm VW]
methane = reference	C_1H_4	802.82	800.35	1	(ref)	(ref)	(ref)	170
n-butane (gas)	$C_1H_{2.5}$	664.6	665.3	0.625	−1.60	−0.61	0.00	261
naphtha (liq)[3]	$C_1H_{2.286}$	637.9	639.1	0.571	−2.15	−0.88	0.00	299
gasoil[4]	$C_1H_{1.88}$	592.7	593.8	0.470	−1.90	−0.90	0.00	327
hydrogen	H_2	241.56	244.72	0.5	+3.84	+1.93	−0.80	445
carbon monoxide[5]	C_1O_1	282.80	283.80	0.5	+4.00	+0.30	+9.50	640
coal syngas[6]	$C_1H_{2.68}O_{1.26}$	475.8	480.8	1.30	+9.32	+2.19	+7.47	76
methanol (gas)	$C_1H_4O_1$	674.2	672.0	1.5	+5.75	+1.66	+3.84	76

[1] Fictive molecular formulae used to calculate the molar combustion heat *LHV*.
[2] $LHV_{(T_2)}$ is the combustion heat defined at temperature T_2 (see Appendix II).
[3] Liquid n-heptane containing 16 % hydrogen by mass.
[4] Gasoil containing 13.5 % hydrogen by mass.
[5] Pure CO is improper for combustion in GT.
[6] Molar composition: 47 % H_2, 15 % CO, 12 % CH_4, 26 % CO_2 .

(a) A higher fraction of inert (e.g., *syngas fuels*: term *LHV* along with $o/2$ and $n/2$ in parameter q_f).

(b) A higher hydrogen or oxygen content (e.g., H_2-*rich fuels*: term $h/4$; *methanol*: term $o/2$).

Remarkably, besides its unique combustion behaviour, hydrogen develops outstanding energy performances in gas turbines. These merits and especially the zero-CO_2 emission of hydrogen explain the increasing interest for H_2-based primary energy routes into the future power generation world [9, 10]. H_2/CO based syngas fuels containing inerts (MCV and LCV gas fuels) have also interesting performances. However, since mechanical energy is required to compress these gases prior to injecting them into GT chambers, the overall energy balance is, of course, different.

(c) A shorter paraffin chain: CH_4 has the highest $h/4$ data and performs better than the other gaseous paraffins C_nH_{2n+2}. Incidentally, the parameter q_f explains why natural gas features better power output and efficiency than gasoil, despite the slightly lower *LHV* of the latter. Though simple, this reason is scarcely set out in the literature.

3.2.2. Influence of the heat capacity of the combustion gases (Cp^g)

From the equations (3)–(5) and the coefficients listed in *table II*, one can see that:

– the higher Cp^g_{34}, the higher the power output, due to the relation (22a): $W_T = n_g(H_3 - H_4) = n_g Cp^g_{34}(T_3 - T_4)$, but:

– the higher Cp^g_{34}, the lower the GT efficiency: this comes from the increase in T_4 (and thus in H_{g4}) caused by a higher Cp^g (see equation (33)), hence less heat is converted into mechanical power.

Both effects explain the higher power output but lower efficiency of CO as a fuel with respect to H_2 (*table III*). Indeed, the concentration ratio (CO_2/H_2O) in the combustion gas, which reflects the C/H ratio of the fuel, impacts on the value of Cp^g, as $Cp^{H_2O}_{34} \approx 0.76 Cp^{CO_2}_{34}$. Whence again the flattering efficiency data developped by both H_2-rich fuels and LCV (N_2-rich) syngas as $Cp^{N_2}_{34} \approx 0.70 Cp^{CO_2}_{34}$.

3.2.3. Influence of the combustion heat of the fuel (*LHV*) on turbine and compressor behaviour

A well-known fact of turbomachinery theory [11] is that η_C (respectively η_T) is a function of the couple of parameters π and T_1 (respectively π and T_3). However, due to the large air excess, the gas flow in a GT is hardly affected by the fuel nature: passing from NG to an MCV fuel causes a minute increase in n_g (and thus in π: see Section 3.3.4) which slightly improves η_T and does not virtually degrade η_C. But for *LHV* data lower than ca. 150 kJ·mol^{-1} (i.e. 7 000 kJ·Nm^{-3}) [12], the

rise in n_g and π becomes so high that the surge limit of the compressor can be reached. This risk is magnified at low ambient temperatures where the compressor must handle higher air mass flows (equation (14)). To prevent compressor surge, it is mandatory to bleed air from the compressor discharge, which entails a dramatic drop in GT performances. However, air bleed is no more a drawback if the bled air is efficiently used to feed, for instance, a gasification unit. Pressurized gasifiers of coal, petroleum residue or biomass consume either compressed *air* (in Air Blown Gasification cycles) or compressed O_2 (in Oxygen Blown cycles) [13]. Such "air integration" raises the overall electrical efficiency of the whole installation which is termed IGCC, the word "integration" applying to both the air and syngas exchanged between gasifiers and CCGT. The *integration factor* is precisely the ratio between the air mass extracted from the GT compressor and that consumed by the gasification unit.

3.2.4. Impact of fuel purity [14]

Four main features make stationary gas turbines sensitive to various forms of fatigue and corrosion (thermal fatigue; hot, type I and II corrosion; fatigue-corrosion; stress corrosion cracking):

– the direct crossing of the turbine path by combustion gases, especially in presence of degraded fuel or air qualities,

– the strongly oxidative conditions (high oxygen excess),

– the policy of minimum cooling of hot mechanical parts, dictated by cycle efficiency considerations,

– the large size of rotating buckets which entail high centrifugal stresses,

– the strong temperature/stress transients entailed, within some operation profiles, by fast start-up and load changes.

Dust-bearing fuels (e.g., blast furnace gas) or ash-forming fuels (e.g., heavy oil) result in solid particles crossing and partly depositing in the turbine, which (i) progressively impairs aerodynamic efficiency and degrades η_T, (ii) restricts the passageway between partition vanes and (iii) may cause erosion and/or corrosion of hot gas path parts.

3.2.5. Specific enthalpy of fuel

The term e_{hf} already mentioned (equation (7)) gives the impact of fuel temperature on GT efficiency. It affects efficiency (equation (3)), but not W_{GT} (equation (2)) as this heat is recovered in the turbine.

From equation (7) it is evident that the term e_{hf} decreases (and thus GT efficiency increases) in the following cases:

– if the fuel *LHV* increases (less fuel will be injected and less sensible heat will be consumed),

– if the fuel temperature (T_8) increases: *natural gas* can be preheated precisely to improve cycle efficiency; *heavy oil* must be preheated to reduce its viscosity; a coal-derived *syngas* can be delivered by a Hot Gas Clean-Up unit, etc.

3.3. Further, non fuel-related considerations

In fact, equations (3)–(5) are not limited to fuel changes but are still valid for any cycle alteration, provided the resulting *changes in the 8 base-variables are small* and keep the couple (k_T, k_C) virtually constant.

3.3.1. Influence of ambient conditions

When ambient temperature drops, both power output and efficiency improve as shown by equations (3) and (4): terms $-k_T\,dT_1/T_1$ and $-(k_C-\gamma)\,dT_1/T_1$, respectively, whence the "evaporative air cooling" [15] or "air chilling" [16, 17] processes intended to raise power output and efficiency by hot weather.

3.3.2. Effect of firing temperature and pressure ratio

The coefficients contained in *table III* show that T_3 has a smaller influence on gas turbine efficiency than on power output. In contrast, the effect of pressure ratio π is minute on power output but strong on efficiency [8]. These trends comply with basic GT theory: in an ideal Brayton cycle, η_{GT} depends on π and not on T_3 (equations (37) and (38)).

3.3.3. Effect of air pollution through compressor efficiency

Although the ambient air is filtered before entering the air compressor, some fine particles and organic contaminants tend to deposit on compressor blades during operation, to reduce compressor efficiency η_C and to degrade thus GT output: coefficient ($k_C\alpha$) in equation (3) and GT efficiency: coefficient $(k_C-\delta)\alpha$ in equation (4). This is why periodical cleaning (off-line or on-line washing) of the compressor is needed for the retention of machine performances [18].

3.3.4. Coupling between gas flow n_g and compressor pressure ratio π

The variables π and n_g are not independent. Indeed, the aerodynamic choking of the combustion gas flow on the first stage GT partition vanes allows to write [19]:

$$\frac{P_3}{m_{g3}T_3^{0.5}M_{g3}^{-0.5}} = R^{1/2}\left\{f\left(k_3^g\right)\right\}A_{PV}^{-1} = R^{1/2}\left\{\left(k_3^g\right)^{1/2}\left[\frac{2}{k_3^g+1}\right]^{\sigma}\right\}A_{PV}^{-1} \quad (8)$$

where A_{PV} is the overall free passage area between the first stage partition vanes; k_3^g is the ratio of the heat capacities of the combustion gas at point 3 ($k_3^g = Cp_3^g/Cv_3^g$); σ equals $(k_3^g+1)/(k_3^g-1)$. The function $f\ (k_3^g)$ is equivalent to $(Cp_3^g)^{0.107}$ around T_3.

Note 1. – To account for the actual gas flow crossing the partition vanes, one should consider here the point 3′ of the "true cycle" (*figure 1b*) and not the point 3 of the "ISO-equivalent cycle" (*figure 1c*), but the difference is small.

Since $P_3 \approx \pi P_1$ with $P_1 = \text{const}$ and $n_{g3} = m_{g3}/M_{g3}$, one can write, for a given machine:

$$\pi \approx K n_{g3} M_{g3}^{1/2} T_{3'}^{1/2} \left(Cp_3^g\right)^{0.107} \quad \text{or}$$
$$\frac{d\pi}{\pi} = \frac{dn_{g3}}{n_{g3}} + 0.5\frac{dM_{g3}}{M_{g3}} + 0.5\frac{dT_3}{T_3} + 0.107\frac{dCp_3^g}{Cp_3^g} \quad (8')$$

Therefore, any change in n_{g3} (due to fuel or any other cause) entails a proportional change in π, which has, however, a limited effect on W_{GT} and η_{GT} as equations (3) and (4) contain not π but $(\ln \pi)$.

3.3.5. Effect of the cooling air flow (n_{ar}) on GT efficiency

Thanks to equations (8′), (3) and (4), it is possible to assess the loss in performance caused by the diversion of compressed air to cool turbine hot parts. Let us consider the same gas turbine as above, burning methane at base load and let us assume, for instance, that one can suppress the cooling air flows and that this represents a fraction r of the global air flow. At base load, the gas flow at the outlet of the first stage partition vanes ($n_{g3'}$) will be multiplied by $(1+r)$ and one will consume r time more fuel to keep $T_{3'}$ constant as the GT cycle control criteria is $T_{3'}$ and not T_3 which is a virtual notion. Therefore, since n_a stays constant:

$$\frac{\Delta FAR}{FAR} = r$$

whence

$$\frac{\Delta n_{g3}}{n_{g3}} = \Delta(q_f FAR) = r FAR \quad (\text{as } q_f = q_{CH_4} = 1)$$

Moreover, equation (8′) shows that π will experience the same relative increase as n_{g3}. As a net result of both n_{g3} and π increase, equations (3) and (4) predict the following performance changes at constant firing temperature:

$$\frac{dW_{GT}}{W_{GT}} = k_T\, d(q_f FAR) + (k_T\beta - k_C\alpha)\frac{d\ln\pi}{\ln\pi} = k_T r FAR + \varepsilon$$
$$\frac{d\eta_{GT}}{\eta_{GT}} = (k_T - 1)\, d(q_f FAR) + (k_T\beta - k_C\alpha + \alpha\delta)\frac{d\ln\pi}{\ln\pi} = k_C r FAR + \varepsilon'$$

This extremely simplified approach assumes that k_T stays unchanged, which in fact leads to undervalue $d\eta_{GT}$. Indeed, the efficiency of the expansion turbine (η_T) will also increase, since the suppression of cooling air admixture in the various turbine stages will (i) increase the fraction of "working fluid" and (ii) reduce flow turbulence and associated exergy losses. As the fuel–air ratio *FAR*, the coefficient k_T and the percentage of cooling air r increase for the more advance GT's, there is an increasing incentive to save cooling air. On the combustion side, a further benefit is that both the combustion richness φ_{rz} and the NO_x emission will be virtually unaffected. These reasons justify the development of new turbine cooling concepts in which cycle-air is replaced by steam flowing within an external loop [20].

3.3.6. Effect of exhaust gas temperature on the efficiency of a combined cycle

While a moderate increase in compression ratio π improves η_{GT}, an increase beyond a certain point may adversely affect the global efficiency of a combined cycle without additional firing. Let T_5 denote the temperature of the combustion gas leaving the HRB (i.e. in the CCGT stack), η_{ST} the overall steam cycle efficiency and HU_{ST}, the heat utilised in the steam cycle. Then η_{CCGT}, the CCGT efficiency can be written:

$$HU_{ST} = n_{g4}Cp_{g4}(T_4 - T_5) \equiv n_{g4}Cp_{g4}(T_4 - T_1)\frac{T_4 - T_5}{T_4 - T_1} = Hex_{GT}\frac{T_4 - T_5}{T_4 - T_1} = (Hin - W_{GT})\frac{T_4 - T_5}{T_4 - T_1}$$

$$\eta_{CCGT} = \frac{W_{GT} + W_{ST}}{Hin} = \eta_{GT} + \frac{\eta_{ST} HU_{ST}}{Hin}$$
$$= \eta_{GT} + \eta_{ST}(1 - \eta_{GT}) \frac{T_4 - T_5}{T_4 - T_1}$$

Since $T_5 > T_1$, the ratio $(T_4 - T_5)/(T_4 - T_1)$ decreases when T_4 decreases and so does η_{CCGT}. A closer analysis taking account of the dependency of η_{GT} on T_4, shows that η_{CCGT} displays a (flat) maximum when π increases. This is why aeroderivative turbines (higher π, lower T_4) do not display better CCGT performance than heavy duty machines [21].

4. FUELS AND COMBUSTION SYSTEMS

4.1. The different types of combustion systems

Besides *catalytic combustion* [22], there are presently two main combustion technologies for GT's, which are *diffusion flame* (or "non-premixed flame") and *premixed flame* combustion [23, 24].

Common features of diffusion and premix combustion in stationary GT's, as compared with boilers or reciprocating engines, are as follows:

– quasi-adiabatic combustion with air already heated by the compression process: 300–400 °C, depending on π,

– pressurised, continuous-flow, steady regime, static chamber-geometry combustion,

– strong molecular dissociation and high concentrations of radicals in the flame front, which efficiently propagate the combustion reaction chains thanks to very fast turbulent diffusion,

– auto-ignition is neither required nor desirable, as initial light up is done by spark ignition,

– flame propagation ability is however required (suitable couple of UFL/LFL data of the fuel),

– large excess of air (overall combustion richness $\varphi_{3''}$ of ca. 0.4–0.5, virtual richness φ_3 around 0.3–0.4) with however a fraction of air subtracted (in most designs) from the combustion usage to cool liner walls,

– medium pressure level (10–15 bar for Heavy Duties and to 30 for aeroderivatives),

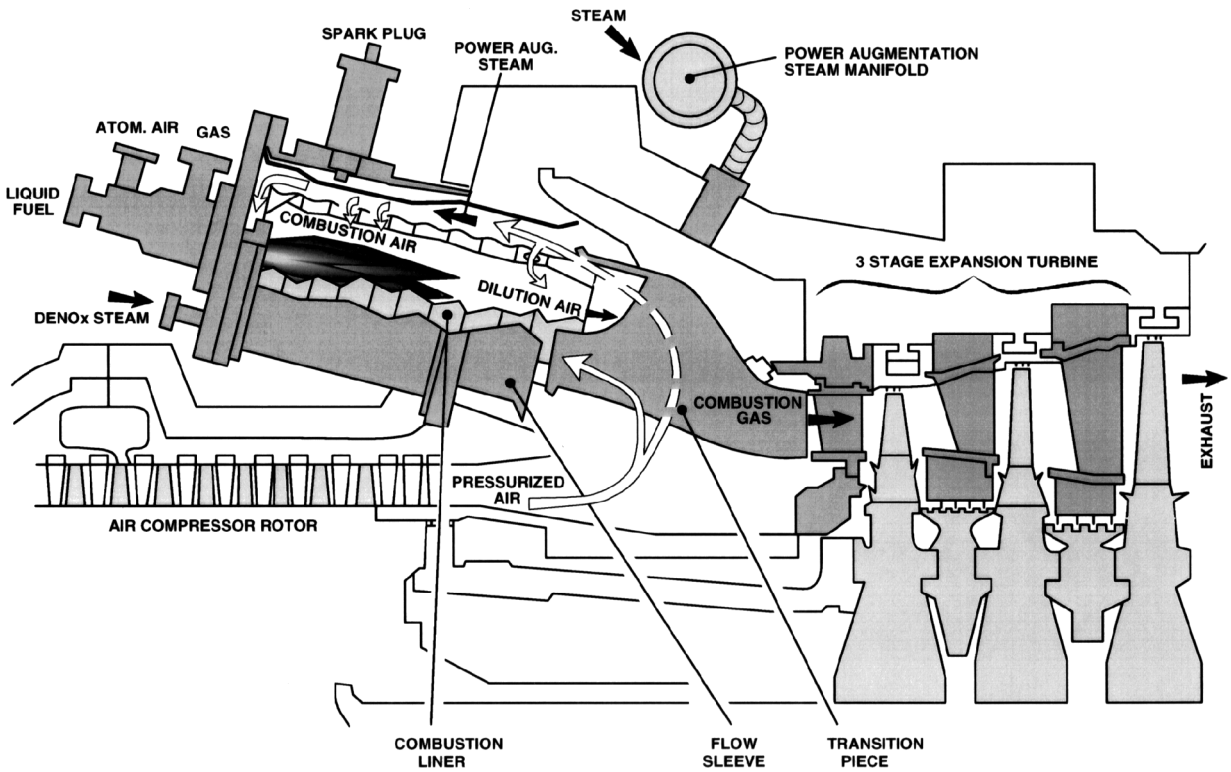

Figure 2. Cross-section of a Heavy Duty GT with two steam injection modes.

– short residence time in the flame, of a few milliseconds (too heavy liquid fuels cannot be burnt),

– high turbulence developing fast fuel/air mixing rates,

– strong flame stabilisation (intense swirl and hot gas recirculation) rendered mandatory by high gas speed which largely exceeds the turbulent combustion speed Uc_t [25],

– possibility of air-assisted atomisation for liquid fuel (to control soot emission) [26, 27].

Note 2. – GT flames are extremely turbulent so that the "reaction zone" is delocalised over a large volume of the combustion liner. But, for simplicity's sake, it is practical to speak about a "flame front".

4.2. Diffusion flame combustors and multifuel capability

4.2.1. Main features

In diffusion flames, *fuel and air mix at the same time and same place as they react*. The specificities of diffusion flame combustors are (*figure 2*):

– gaseous and liquid fuels are burnt on the same principle, based on direct fuel injection,

– flame front is essentially heterogeneous in fuel strength, with high internal temperature gradient and thus intense, stability-enhancing recirculation of reacting gas in the primary zone,

– the stoichiometric zone is very hot (typically 2 000–2 300 °C, which is ca. 150–200 K above atmospheric flames),

– auto-ignition in steady operation regime is not an essential risk (no premix prior to combustion).

4.2.2. Fuel flexibility

This essential gradient of richness and temperature provides some kind of "self-piloting effect" at the microscopic scale which can be interpreted as follows: should combustion kinetics weaken at a given flame spot due to a too low (respectively a too high) fuel strength, it would be immediately "rescued", through turbulent diffusion, by adjacent cells having higher (respectively lower) fuel strength. This explains the high "robustness" of diffusion flames and:

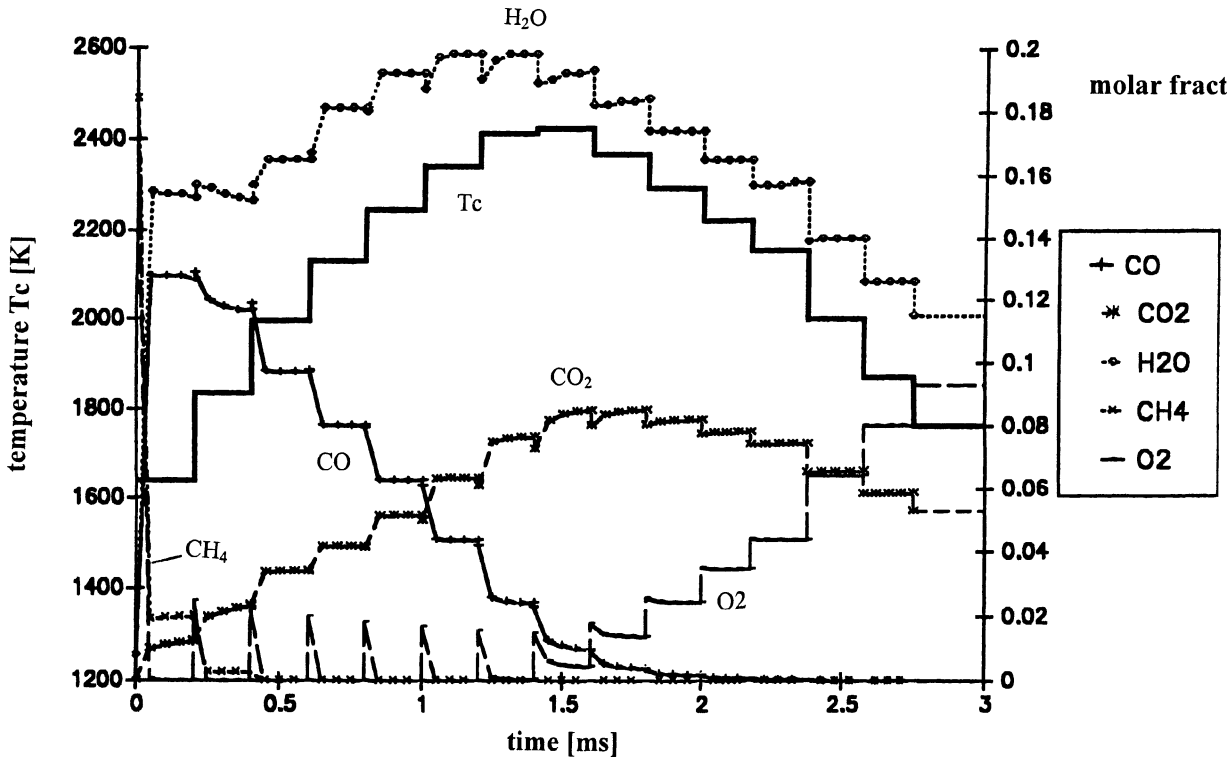

Figure 3. Species concentrations along the combustion liner.

TABLE IV
Impact of liquid fuel properties on combustion and further GT processes.

Fuel property trend	Effects on combustion	Ultimate effects
higher viscosity	increases fuel droplet size	increases smoke (cenospheres)
higher C/H ratio [26], carbon residue and aromatics content	increases Tc_s generates PAH's	increases thermal NO_x increases soot, UHC, CO
higher sulfur content	conversion of S into SO_2	increases SO_2 and SO_3 emissions raises flue gas Dew Point: HRB
higher FBN	conversion into organic NO_x	increases overall NO_x
content of inert inorganics (Ca, Ni, Al, Fe)	formation of refractory, chemically inert ash	erosion, deposition (fouling the turbine)
content of corrosive metals (Na, K, V, Pb)	generation of low melting-point ash	hot corrosion of turbine parts [14]: *low and high temperature hot corrosion*

– their large fuel acceptance,

– their stability over a wide load range of the chambers,

– the possibility to admix external fluids (steam, water, nitrogen etc.) into the reaction zone in order to reduce NO_x while incidentally augmenting GT power output (increase in n_{g3}).

All these features explain the universality of diffusion-flames in gas turbine applications and account for their dual-fuel capability as well. The fuel spectrum of Heavy Duty GT's, much larger than that of Diesel engines, covers a number of liquid fuels and a wide range of HCV–MCV–LCV gas fuels (*table I*). As Heavy Duty GT's create relatively loose combustion requirements, they represent the prime movers of choice in CHP units integrated in industrial plants where process by-products can be used as GT fuels (refineries, steel processing, carbo/petro-chemistry, food industry etc.).

4.2.3. Influence of gas fuel properties

The high combustion temperature and the overall oxygen excess which prevail in GT chambers enhance combustion kinetics, so that the *characteristic chemical time of combustion* (τ_{ch}) is lower than that of turbulence (τ_t, a data practically unchanged from one fuel to another). However, different hydrocarbons feature different *Tc* and τ_{ch} data, which influence NO_x emission and potentially combustion completion (CO/UHC emissions). *Figure 3* shows how the concentrations of chemical species evolve along a combustion liner during the combustion of methane [28].

4.2.4. Influence of liquid fuel properties

Table IV summarises the impact of liquid fuel properties on combustion and other GT processes.

5. FUELS AND GASEOUS EMISSIONS

Emission control has become a major task of the gas turbine industry [29]. Typically, modern GT routinely achieve combustion efficiency as high a 99.99 % at base load with CO and UHC emissions as low as 10 ppm. However, NO_x is becoming a pollutant of increasing concern, as the firing temperature of today's machines is gradually raised for performance enhancement. Another essential feature of GT emissions lies in the fact that NO_x, on one hand, and (CO + UHC), on another hand, undergo opposite changes versus firing temperature and thus versus load (*figure 4*).

5.1. Emission control within diffusion flame combustion

5.1.1. Basic notions

Historically, the first GT combustion systems were based exclusively on diffusion flames which involve direct fuel injection and feature broad spread of fuel/air ratio throughout the reaction zone. Diffusion flames develop, therefore, high peak temperatures (*figure 5*) and high emissions of *thermal* NO_x (the highest at base and peak load) but provide in counterpart stable and efficient

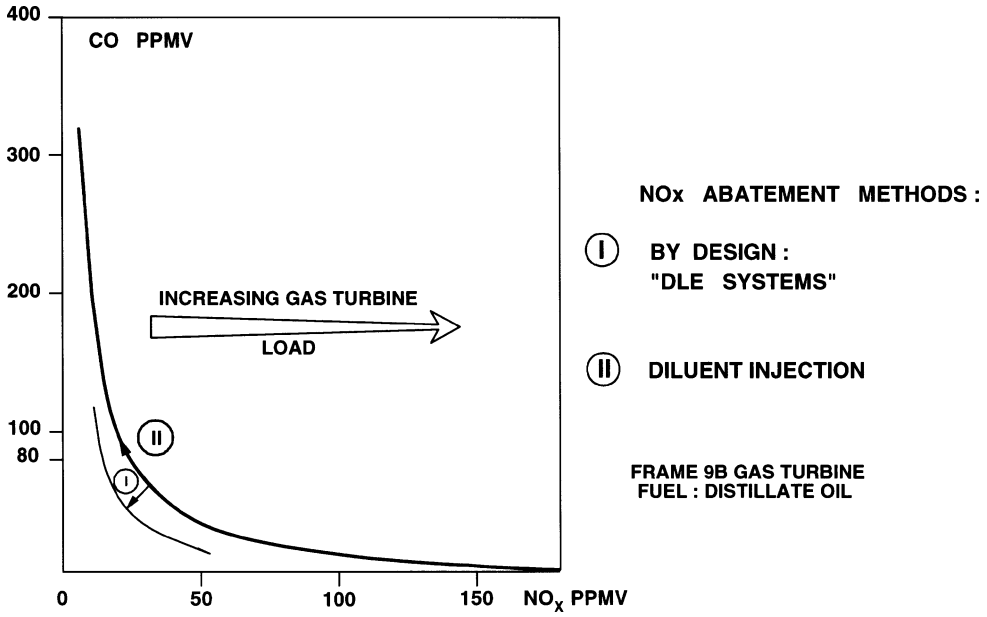

Figure 4. Correlation between NO_x and CO.

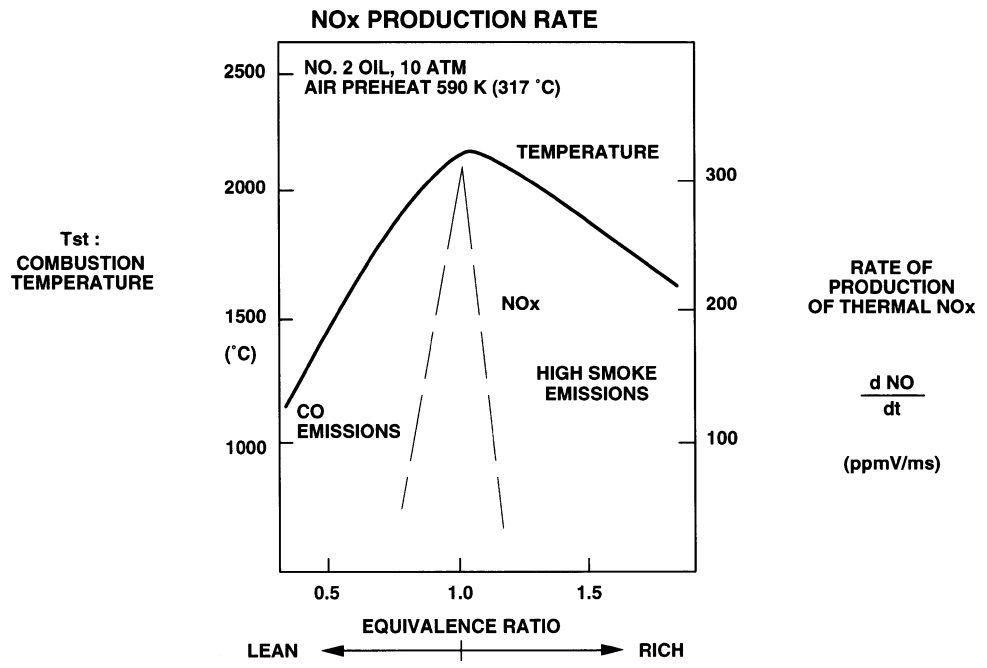

Figure 5. Emission kinetics versus combustion richness.

combustion over a large GT operation envelope. The three basic mechanisms of non-organic NO_x, i.e. the Zeldovich'es, prompt NO and N_2O routes, have been abundantly described elsewhere [30–32].

A basic NO_x emission determinant is the *adiabatic, stoichiometric combustion temperature* (Tc_s), which is the maximum theoretical temperature reached in the combustor, taking account of molecular dissociations

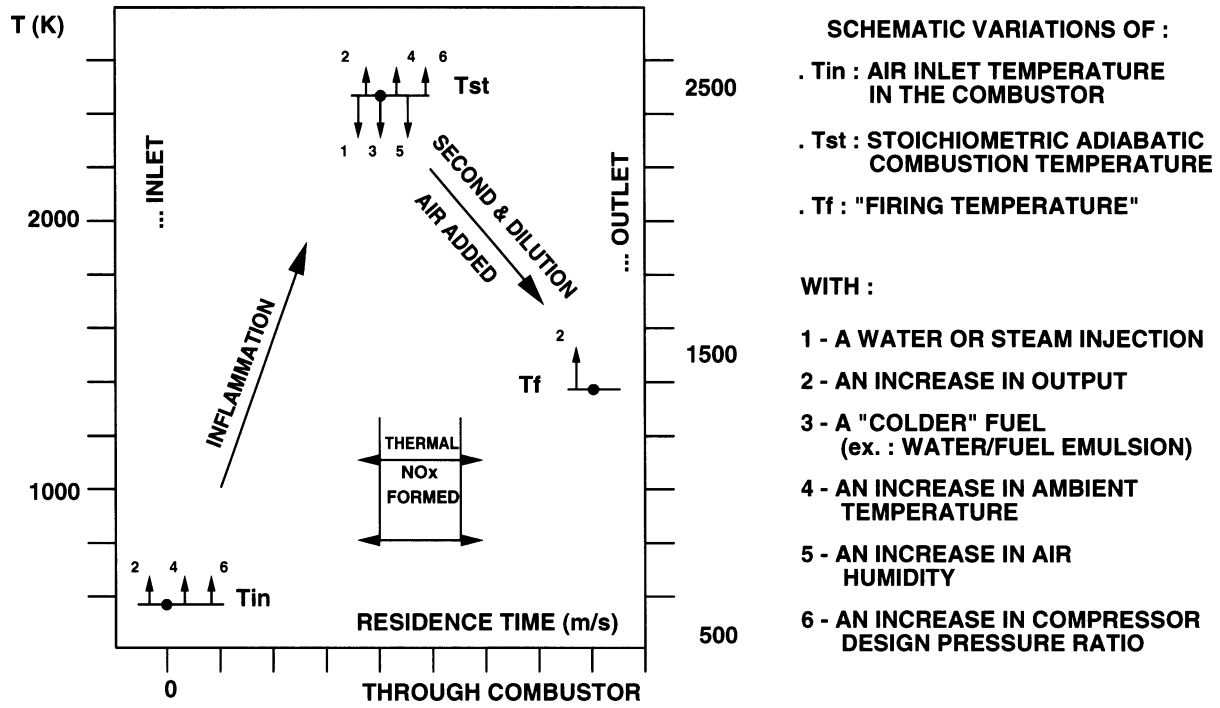

Figure 6. Reaction route in a gas turbine combustor.

which are promoted at high temperature but neglecting radiative losses. Tc_s enables the prediction of NO_x changes versus ambient and operational conditions (*figure 6*) and the calculation of NO_x indices of GT fuels [33, 34].

Another form of NO_x called *organic* NO_x is added to thermal NO_x when the fuel contains chemically combined nitrogen, termed *fuel bound nitrogen*. This type of NO_x forms as FBN atoms, which are much more reactive than N_2, combines with O atoms in the reaction zone. Fuels with significant FBN contents are: (i) heavy distillates, (ii) heavy oils and (iii) some syngas products, depending on their purification process. *Figure 7* shows that the conversion rate of FBN to NO_x declines when FBN increases [35] as there is a competing mechanism consisting in the recombination of nitrogen atoms ($N\cdot + N\cdot \rightarrow N_2$), which has a second-order kinetics with respect to FBN and is enhanced by high FBN.

5.1.2. NO_x emission indices of fuels

The notion of Tc_s is a powerful tool to compare the thermal NO_x generated by gaseous and liquid fuels. Appendix IV shows that the NO_x emission associated with a fuel $C_cH_hO_oS_sN_n$ (which is assumed FBN-exempt) can be written:

$$NO_x = k P_2^m \exp\left[\frac{k'(LHV_{(T_1)} + \omega H_{a2} - E^{dis})}{c\check{C}p^{CO_2} + \frac{h}{2}\check{C}p^{H_2O} + \left(\nu\omega + \frac{n}{2}\right)\check{C}p^{N_2}}\right] \quad (9)$$

where $\omega = c + h/4 + s - o/2$.

E^{dis} is the energy consumed by the equilibrated dissociation of the reaction products in the flame front and $\check{C}p^i$ is the average heat capacity of species i between T_1^0 (288 K) and 2 350 K. E^{dis}, which refers to one fuel mole, remains very small with respect to *LHV* (less than 10^{-3}).

Formula (9) enables a parametric analysis of fuel influence on NO_x emission: *table V* shows a number of fuel properties affecting the NO_x index data (INO_x) of fuels (*table III*).

Figure 8 shows the NO_x indices of various fuels calculated at constant ambient conditons, combustor design and thermal load, taking methane as reference fuel.

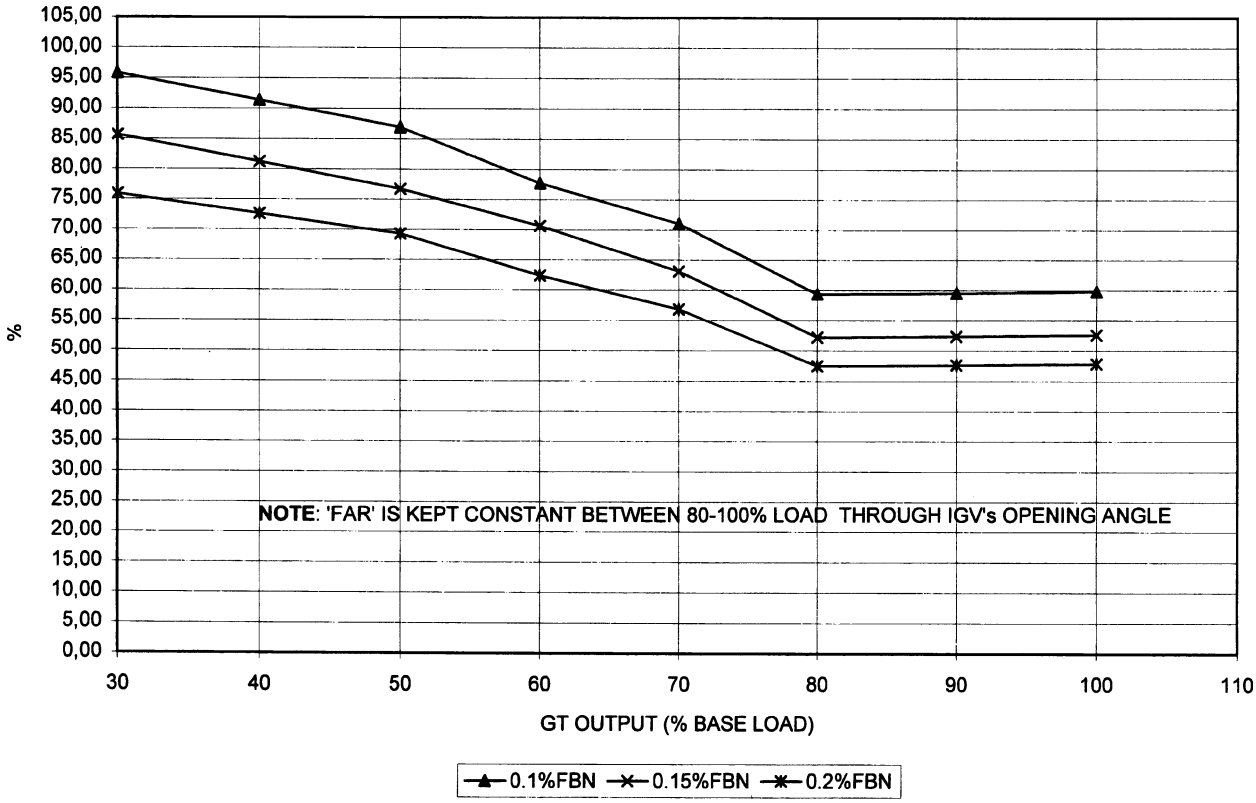

Figure 7. Conversion rate of FBN into NO_x in function of GT output.

TABLE V
Impact of various molecular properties of fuels on NO_x index.

Fuel property or thermal effect	Effect on INO_x (equation (9))	Example (reference fuel: CH_4)
Molar combustion heat (*LHV*)	Higher *LHV* increases NO_x	Alcohols have lower *LHV*, so lower INO_x
Stoichiometric consumption of oxygen (ω)	Lower ω data increases INO_x	H_2 and CO have higher INO_x INO_x aromatics > olefins > paraffins
Molecular formula ($C_cH_hN_nO_o$)	Smaller $h/2$ data increases NO_x	INO_x of C_cH_h increases if h/c decreases: NG < propane < butane < naphtha < gasoil
Diluents (N_2, CO_2 etc.)	High inert content decreases INO_x (term n at denominator)	Syngas, blast furnace gas, lean NG
Molecular dissociations	Higher E^{dis} tends to decrease INO_x (see Note 9 in Appendix VI)	Effectiveness of diluent injection falls off at high RI levels (less dissociation)

5.1.3. NO_x emission in "mixture" combustion

"Mixture combustion" means that two fuels are burnt simultaneously in a gas turbine. They may be two gaseous fuels (not premixed with each other) or one gaseous plus one liquid fuel. For instance, if commercial natural gas is available in insufficient quantity for base load operation, it can be complemented by gasoil stored in the plant.

As shown in Appendix V, the NO_x data of a two-component mixture follows a "geometric mean" law in function of both fuel NO_x data. If x_j denotes the mole

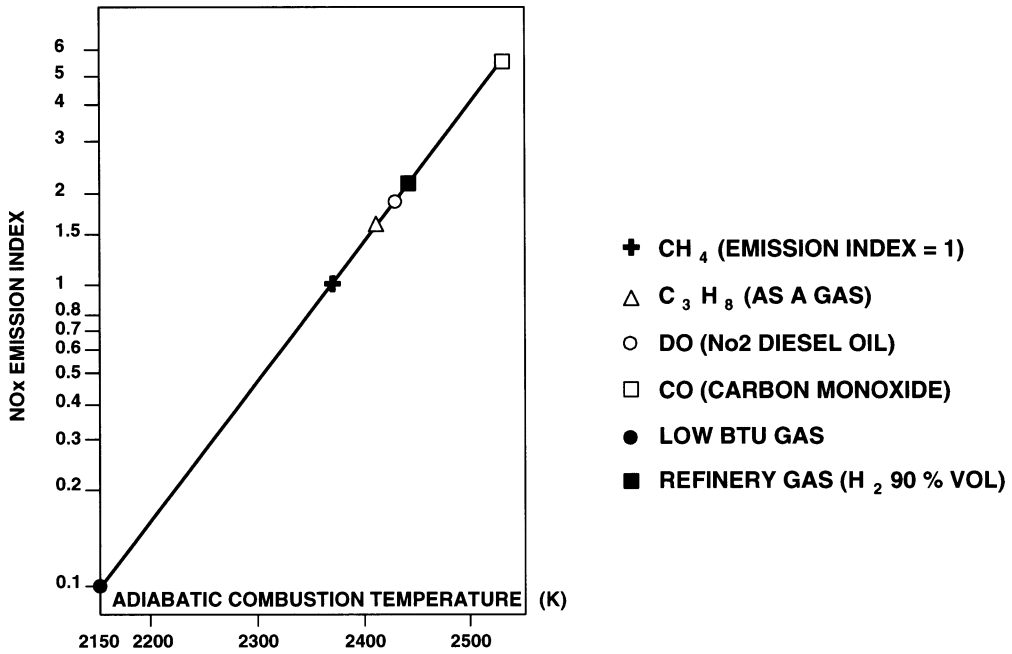

Figure 8. NO_x emission index data of various fuels.

proportion of fuel j in the mixture, this original result can be summarized by the simple relation [36]:

$$NO_{x_{\text{mixture}}} = (NO_x)_1^{x_1} \cdot (NO_x)_2^{x_2} \tag{10}$$

5.2. Non fuel-related factors

Equation (9) can be used to assess effects of further cycle changes, namely ambient conditions (*figure 6*):

(a) Inlet air temperature. Due to the term H_{a2}, NO_x increases if T_2 increases, which results from an increase in T_1. Indeed, at constant atmospheric pressure, equations (8′), (15) and (32) lead to:

$$\frac{dT_2}{T_2} = \left[1 - \frac{R}{\eta_C Cp_a}\right]\frac{dT_1}{T_1} \approx 0.67\frac{dT_1}{T_1}$$

so that

$$\frac{dH_{a2}}{H_{a2}} = \frac{dT_2}{T_2 - T_1} \approx 2\frac{dT_2}{T_2} = 1.34\frac{dT_1}{T_1}$$

(b) Pressure. The pressure P_2 depends not only on the ambient pressure P_1 but also on fuel (as per equations (8′) and (2)). However, the effect is small. In fact, one can take $m \approx 1/2$ in equation (9).

(c) Air humidity. Introducing air humidity (so far neglected) in equation (49), leads to an altered form of equation (9):

$$\frac{NO_{x_{(w)}}}{NO_{x_{(w=0)}}} = \exp\left[-\frac{k'(1+\nu)\omega \check{C}p^{H_2O} w}{c\check{C}p^{CO_2} + \frac{h}{2}\check{C}p^{H_2O} + \left(\nu\omega + \frac{n}{2}\right)\check{C}p^{N_2}}\right] \approx \exp(-kw) \tag{11}$$

where w is the absolute air humidity defined here as the ratio (mole of H_2O in air/moles of dry air). This is the exponential form of the humidity-correction formula often used [37].

5.3. Wet control of thermal NO_x within diffusion flame combustion

With diffusion flames, the only effective route to reduce thermal NO_x, often termed "*wet control*", consists in injecting an inert fluid or "diluent" in order to reduce Tc_s. Such diluent (denoted d hereafter) can be water or steam (the most widespread diluents) but also N_2 or even CO_2. Thanks to their intrinsic stability, diffusion flames accept the admixture of considerable quantities of diluents or inerts.

5.3.1. Effect of diluent injections on thermal NO_x [38]

Appendix VI dealing with the injection of water or steam on thermal NO_x leads to the equation:

$$(NO_{x_{RI}}) = (NO_{x_{RI=0}})\left\{1 - RI_{rz}\ln(NO_{x_{RI=0}}) \cdot \left[\frac{Lv_d - H_{d9}}{A} + \frac{Cp^d}{B}\right]\right\} \quad (12)$$

where:

– RI_{rz} is the injection rate of diluent d in the reaction zone (or flame front) (moles of diluent/moles of fuel),

– Lv_d is the latent vaporisation heat of the diluent ($Lv_d = 0$ for steam),

– A and B are parameters independent of RI but functions of: T_2 (thus of π); fuel composition; LHV and combustion stoichiometry.

Figure 9 illustrates the linear decrease in NO_x with water injection.

At this stage, it is important to stress that the effective fraction of diluent for NO_x abatement is the one which actually reaches the flame front (hence the notation RI_{rz}). Indeed, the classical steam injection mode (often termed "$DeNO_x$ injection") is performed into the chambers and the steam jets aim at the flame front. Now there exists another form of steam injection (termed "*power augmentation injection*", *figure 2*) which is effected at the compressor discharge, i.e. upstream of the chambers. In the latter injection mode, only a fraction (F_{rz}) of the steam is actually routed to the flame front whilst the rest follows the main air stream and goes through the cooling louvers and dilution holes of the liner. In this case, equation (12) shows that, for a given injection rate defined at the injection port (point 9), the NO_x abatement effectiveness is only F_{rz} times that of the "$DeNO_x$ injection" mode [39]:

$$\frac{\Delta[NO_{x_{RI}}]_{\text{Power augmentation}}}{\Delta RI_9} = \frac{F_{rz}\Delta[NO_{x_{RI}}]_{DeNO_x}}{\Delta RI_9} \quad \text{with } F_{rz} < 1 \quad (13)$$

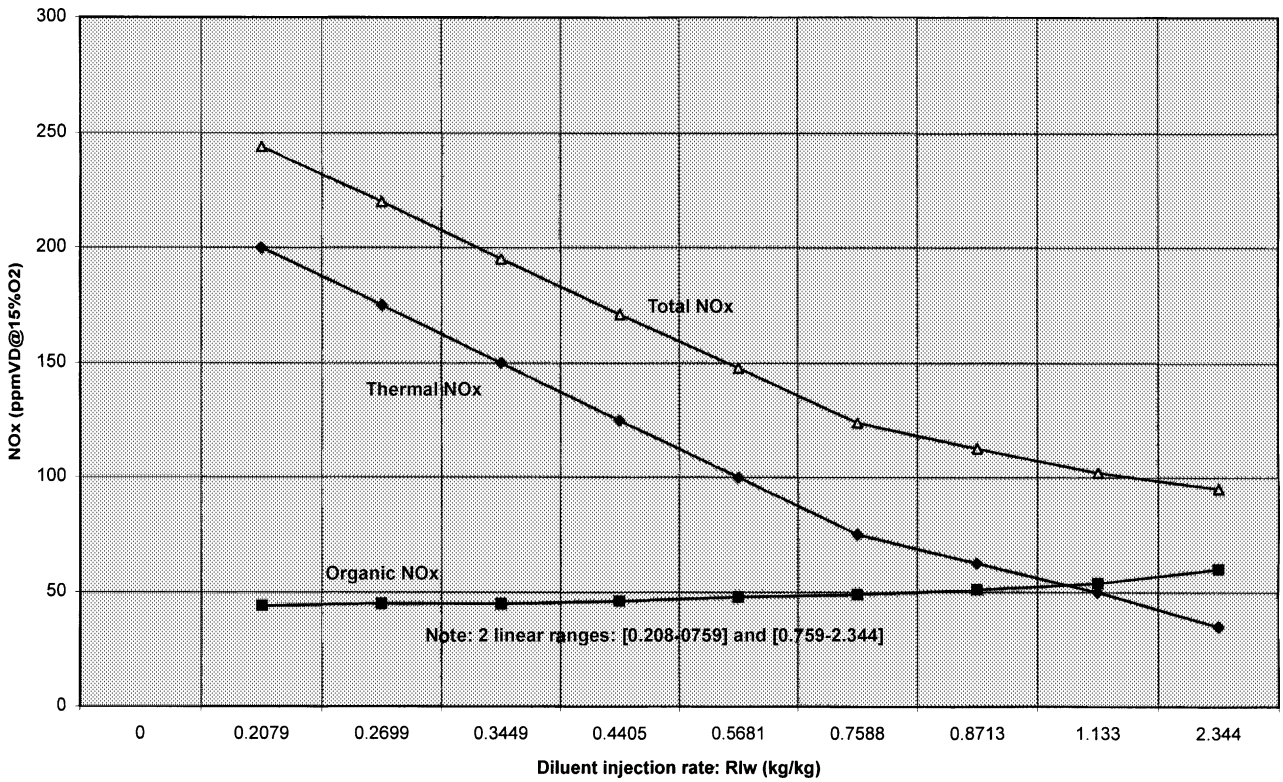

Figure 9. Effect of water injection on the emission of thermal and organic NO_x (0.2% FBN).

However, both injection modes yield the same gains in output and efficiency as shown below.

5.3.2. Effect on energy performances

Appendix VI shows that:

– both steam and water injections increase power as they increase n_g and Cp^g (equation (58)),

– efficiency increases in case of steam injection but declines in case of water injection essentially because the latent vaporisation heat of water is normally not recovered within the cycle (equation (60)).

In addition, the recoverable heat *Hex* stays virtually constant (n_g and Cp^g increase but T_4 slightly declines with actual temperature control curves).

5.3.3. Effect of diluent injection on organic NO_x

Unfortunately, injecting water or steam does not reduce but slightly increases the conversion of FBN into NO_x [39] (*figure 9*). This comes from the fact that (i) the kinetics of organic NO_x are much less temperature-dependent than those of thermal NO_x, and (ii) flame quenching increases flame length, residence time in the flame and moves the flame more downstream in the combustor, i.e. towards leaner zones. Now, the more "oxygenated" the flame, the higher the conversion of FBN to NO_x (Section 5.7).

5.4. The various, non-wet, low NO_x strategies

Since the early 80's, alternative low-NO_x control strategies have been developed [29] (*figure 10*):

(i) change in combustion/dilution air split along the combustor liner,

(ii) "multi-nozzle" combustion in which the flame is split into several smaller flames,

(iii) fuel or air staging to avoid the high temperature band,

(iv) *lean, premixed flames* which develop low combustion temperatures,

(v) catalytic combustion, which is a flameless oxidation process.

Dry low NO_x (DLN) or *dry low emission* (DLE) systems generally combine the first four design measures and presently offer the most successful solutions for natural gas operation.

DLN technologies, like all the "primary" measures, tackle the root causes of NO_x generation and are favoured by gas turbines designers. In contrast, "secondary" or

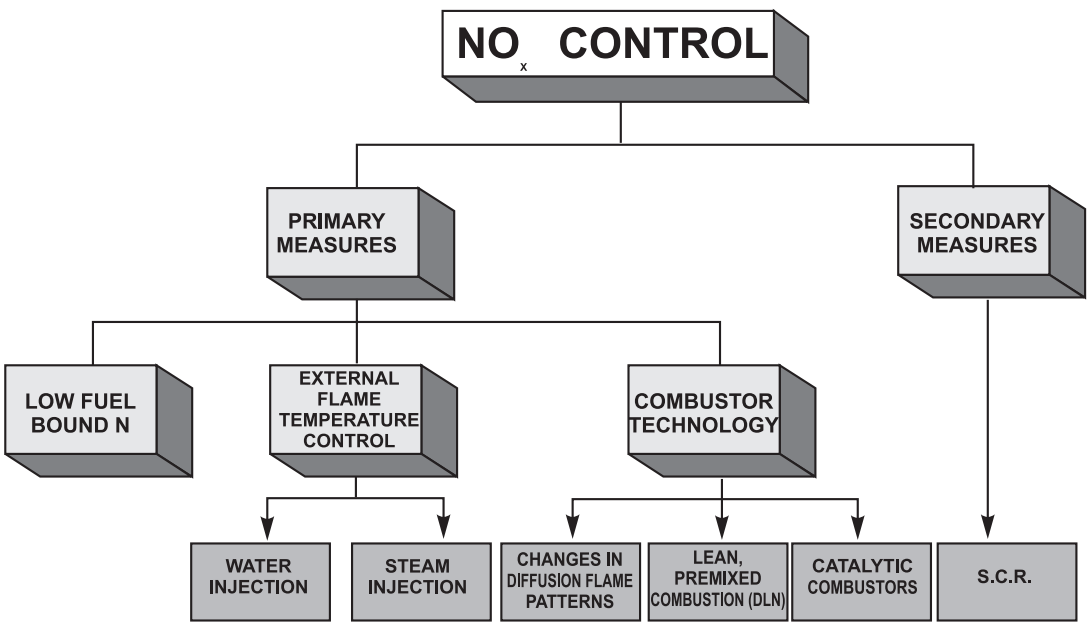

Figure 10. NO_x control strategy routes.

"postcombustion" measures like selective catalytic reduction (SCR) of NO_x and catalytic oxidation of CO/UHC aim to suppress pollutants already formed [40, 41]. Selective noncatalytic reduction (SNCR) processes based on ammonia/urea injections are not applicable to gas turbines as the ranges of temperature and residence time which prevail in GT are not suitable.

Finally, some iron-, manganese- or barium-based additives are sometimes used as "smoke suppressants", i.e. to abate soot particles emitted by some viscous or hydrogen-depressed liquid fuels, thereby reducing the opacity of flue gases [42].

5.5. Dry low NO_x systems [43]

Premix flames differ from diffusion ones in many respects:

– the aim is to develop the leanest and the most homogeneous fuel strength throughout the reaction zone and to generate the lowest Tc_S data (typically 500–600 K below that of diffusion flames),

– due to this flame front uniformity, there is less hot gas recirculation and the "mutual kinetic rescue" between neighbouring reaction cells is weaker (see Section 4.2.2).

Therefore, the global kinetics is more easily weakened (the "radicals pool" is also less reactive) so that a powerful aerodynamic stabilisation is required (usually by vortical or swirl gas/air motion).

Historically, this "lean-premix" route has proven the most consistent technology for thermal NO_x control. Since premix flames are intrinsically less stable than diffusion flames, industrial DLN systems must include all the provisions required to achieve: (i) machine light-up, (ii) load change and (iii) large "turn-over", while operating the reaction zone near the "*weak extinction*" limit at base load. Presently, 25 ppm NO_x seems to become the best achievable control technology (BACT) for low NO_x stationary gas turbines in a number of regions worldwide [44].

The following measures are typical of second-generation GT designs (*figure 11*):

– two-stage combustor with a "primary" and a "secondary" zone,

– lower load range operated on diffusion flame by igniting first the primary, then the secondary zone,

– higher load range operated on premix flame: gas and air are premixed in the primary zone and burnt in the secondary zone, where a pilot flame assists for combustion stability,

– design features to prevent flame retro propagation (flash-back) towards the primary zone.

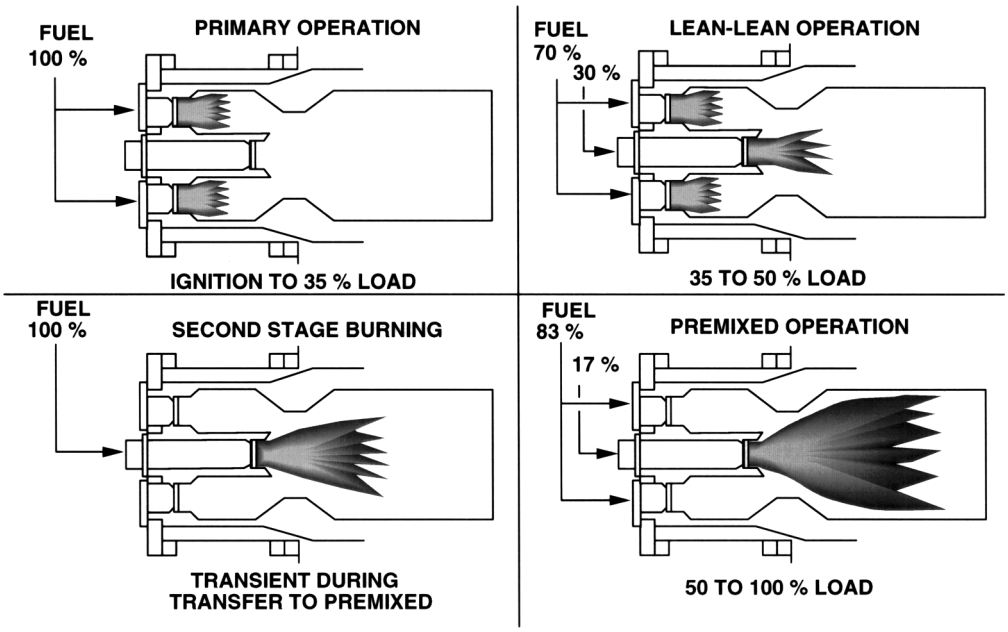

Figure 11. DLN-1 operating modes.

This paper does not aim at reviewing extensively the design and operation of DLN systems, which are described elsewhere [43]. In contrast, it is interesting to analyse the strong interrelationship between fuel and premix-flame combustion and stress the "fuel-specialisation" of DLN systems.

5.6. DLN combustor designs and fuel specificities

DLN combustion chambers based on premix flames must be strictly operated between two borderlines: (i) blow-off and (ii) flash-back. Auto-ignition and deflagration-to-detonation transitions pose further limitations. In all these processes fuel properties which impact on the turbulent speed of combustion (Uc_t) are involved.

(a) Blow-off occurs if Uc_t drops below the speed of the reacting gases (Vc), which tends to push the flame front downstream. This occurs either if gas speed suddenly increases (flow transient) or, more frequently, if combustion kinetics are slowed down by a fuel strength too close to the LFL (weak extinction) which is likely to happen at low machine loads. Weak extinction is frequently preceded by intense thermo-acoustic activity (strong "pressure dynamics") and surging CO/UHC emissions. The accessible power range of premix operation, often called "*turn down*", is thus restricted on the low load side. Turn-down can be widened by resorting to a cycle artefact known as "*bleed heating*" whereby hot air discharged by the GT compressor is recycled at the compressor intake. Bleed heating produces the following changes: it successively increases air inlet temperature T_1; reduces the cycle air flow n_a (equation (14)) and correlatively n_{g3} and π (equation (8)); increases, therefore, firing temperature T_3, as required by equation (3) to keep power output constant. Finally, increasing T_3 requires additional fuel which shifts fuel richness towards the stable-premix region.

The presence of inerts in fuels both depresses Uc_t and increases Vc (increased gas flow) and impairs premix flame stability. Some inerts, like N_2, have on Uc_t a purely thermal or "quench" effect (decrease in Tc_s) while others may have an additional kinetic effect, like CO_2 which has strong extinguishing properties. The slightly positive kinetic effect of H_2O on flame stability (enabled by the reactivity of H and OH) is more than offset by its negative "quenching" effect.

(b) Flash-back occurs if Uc_t locally exceeds the speed of the reacting flow Vc, which tends to pull the flame upstream, towards the premixing zone, the highest flash back risk being in flow boundary layers (near liner walls) where flow speed goes down to zero. Now, Uc_t is strongly tied with the intimate combustion kinetics of the fuel and increases with flow turbulence and fuel richness. The quality of "premixedness" of fuel and air is a paramount quality of DLN designs for two main reasons. Indeed "unmixedness" generate richer, hotter combustion cells which: (i) will generate surplus NO_x in an exponential way [45] and (ii) will become potential sites for flash-back, especially within boundary layers. One can say that one of the greatest challenges faced in DLN systems for advanced GT's lies in the attainment of the most even *FAR* profile along with the minimisation of pilot flame load (*figure 12*) which resorts to inventive, aerodynamically sophisticated and geometrically refined devices (vane-generated swirls, vortices, etc.) [46, 47]. These issues interfer with hot part "lifing" and the control of thermoacoustic effects.

(c) Auto-ignition (AI) is a third limitation of DLN combustion. AI triggered in the flow *bulk* can be caused by the mere level of temperature T_2 or by the radiative heat received from the downstream reacting zone. AI can be also *surface*-triggered (e.g., if particles of carbon-black have deposited on liner walls during previous operation of the primary zone on liquid fuel). AI is characterised by three main data: temperature (T_{AI}), delay (τ_{AI}) and energy (E_{AI}) [48]. In GT combustors, AI risks depend on (i) *temperature*, (ii) *static pressure* and (iii) *time* elapsed between premix and injection into the flame front. Longer chain paraffins have lower T_{AI} and shorter τ_{AI} data than methane [49]. For instance, premixing butane with the air discharged by modern GT compressors featuring high pressure ratio and T_2 data (20 bars, 420 °C), would generate very low τ_{AI} data and increase the risk of self-ignition. In some respect, this minimum τ_{AI} requirement parallels that of spark-ignited engines but fortunately, the lower pressure and temperature levels in GT's are not conducive to detonations. Finally, when burning natural gas, AI events in the premix zone are possible if natural gas contains heavier hydrocarbons, due to the low AIT of the latter. In this respect, it is noteworthy that commercial supplies of natural gas are much less stable in composition than gasoline and gasoil products.

(d) Characteristic reaction time (τ_{ch}). Due to the limited geometric length of the combustion liners, there is a maximum time available to achieve 100 % combustion of the fuel and avoid the release of CO/UHC. Now, some fuels (especially pure CO) have intrinsically

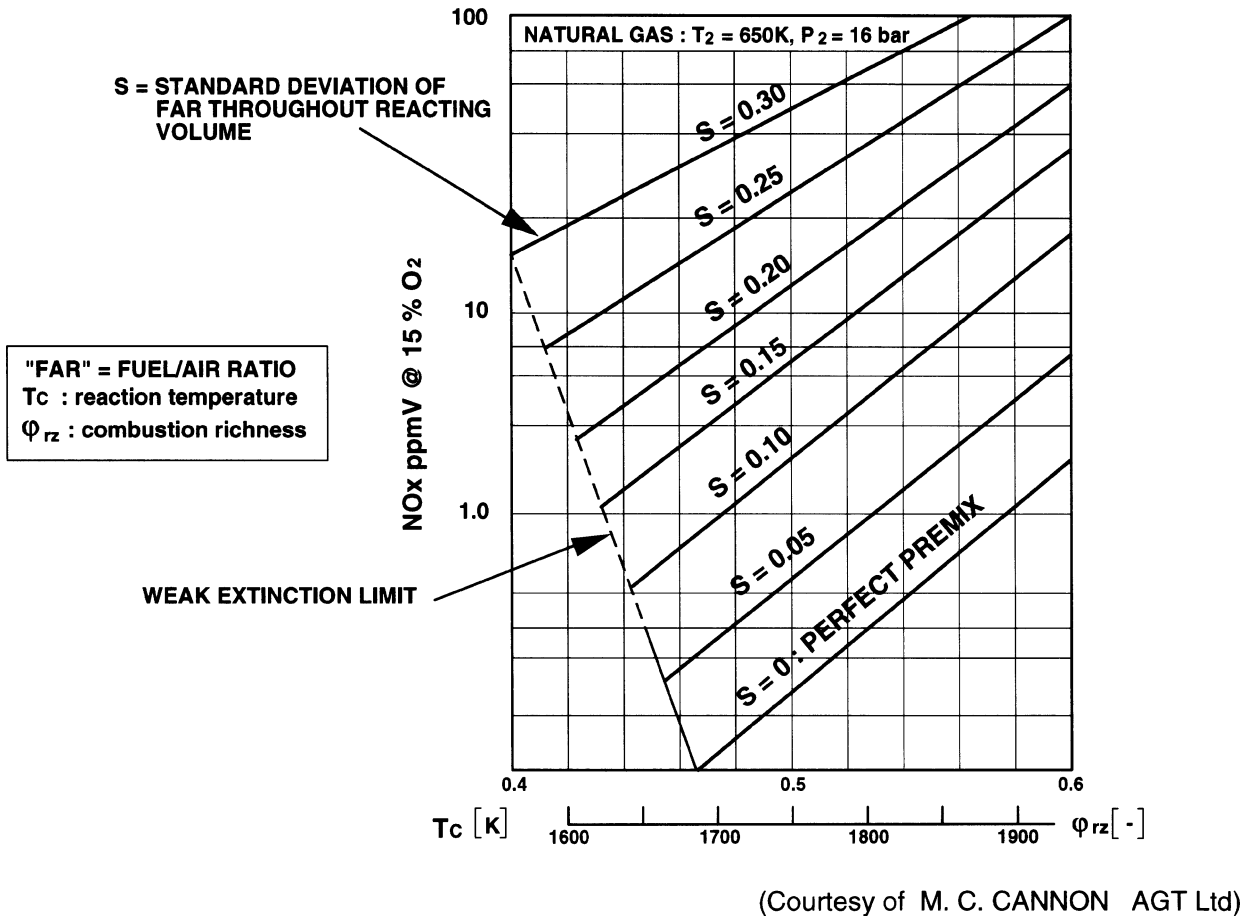

Figure 12. Effect of fuel/air unmixedness on NO_x emission.

"lazy" combustion kinetics or their combustion mechanisms involve a larger number of elementary steps than methane and need more time for completion. For instance, the combustion mechanism of C_nH_{2n+2} involves stepwise fragmentation of the hydrocarbon skeleton prior to forming CO and OH species which are ultimately oxidised into CO_2 and H_2O. As the *Tc* data of premixed flames is much lower than that of diffusion flames, the characteristic time τ_{ch} is increased so that a complete combustion of such fuels is not always achievable within CH_4-specialised DLN concepts. In addition, the imperfect combustion of such fuels can raise the troublesome "yellow plume" syndrome at the stacks of large GT's. Such undesirable plume coloration is associated with the formation of nitrogen dioxide (NO_2) in the flue gases. The yellow-brownish NO_2 results from a partial conversion of the colourless NO in presence of CO/UHC [50, 51].

(e) Deflagration-to-detonation transitions. Hydrogen has a particularly low τ_{AI} data, is prone to catalytic ignition (E_{AI} is reduced by chemisorption/dissociation on metallic walls) and H_2/air premixtures have a high propensity to pass from deflagration to strong detonation regimes, as a result of its high Uc_t and stoichiometric combustion temperature Tc_S. Therefore there is presently no industrial premix technology capable of burning H_2-rich gas fuels. In turn, fuels containing slight proportions of H_2 can be utilized in DLN combustors after some adaptations are made (change in chamber geometry to prevent flash-back [52]). This leaves a challenging investigation field opened (diffusion flames of H_2 generate high NO_x), in consideration of the promising future of H_2-based energy cycles.

In conclusion, while standard diffusion-combustors can handle a wide fuel spectrum, current commercial DLN systems are essentially designed and industrially

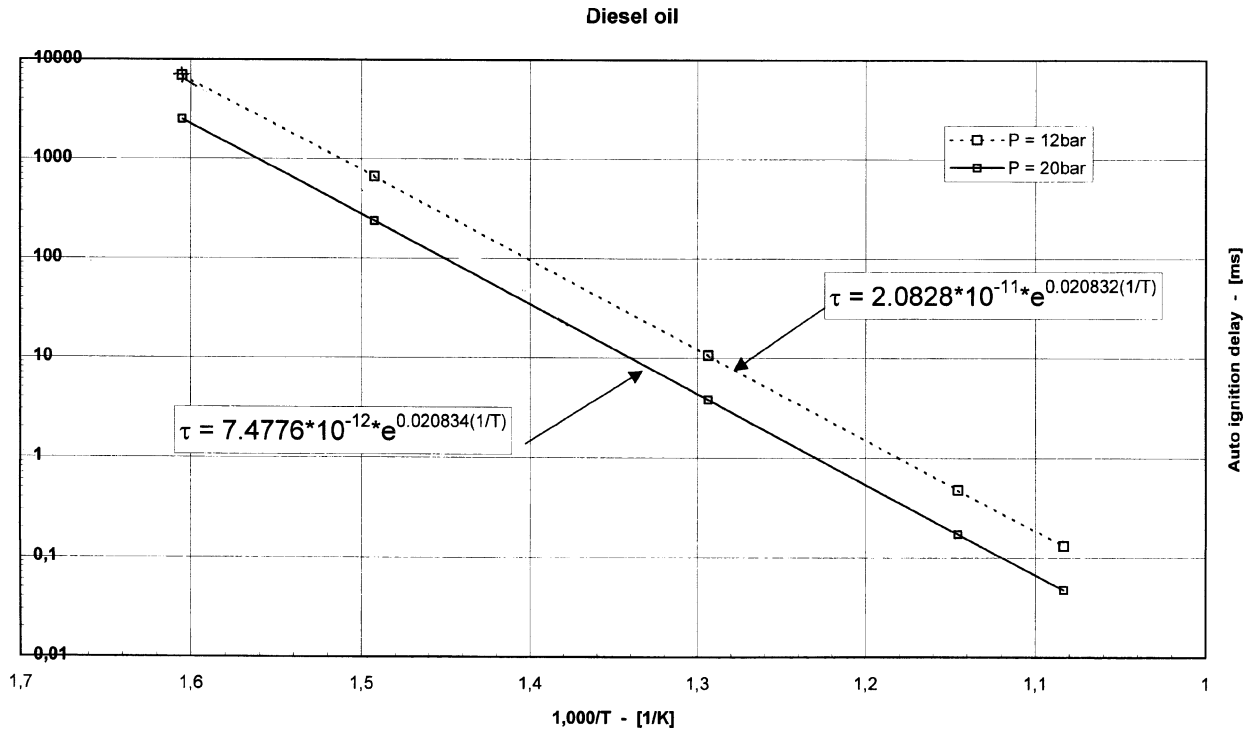

Figure 13. Influence of temperature and pressure on auto ignition delay.

developed to handle "normal" natural gas fuels (containing limited amounts of heavy paraffins, inerts and H_2).

5.7. Dry oil low NO_x combustors

The AI-delay τ_{AI} plays an essential role in the new concepts of premix combustion for liquid fuels ("Dry oil low NO_x" combustors) [53] in which the overall time for atomisation, vaporisation and premixing must not exceed τ_{AI}. Now τ_{AI} not only depends on fuel chemistry but also sharply decreases with temperature and pressure [54, 55] (*figure 13*):

$$\tau_{AI} = A P^n \exp(B/RT)$$

The set of parameters A, n, B depends on the working ranges of temperature and pressure. For Diesel oil, the auto-ignition delay is divided by a factor of 100 when the pressure ratio rises from 12 ($T_2 \approx 620$ K) to 20 ($T_2 \approx 720$ K) in a non-inter-cooled machine (see arrow in *figure 13*). In addition the decrease of τ_{AI} with increasing hydrocarbon chain length, taking butane as reference, can be outlined as follows: *butane* (C_4H_{10}): 1; *n-hexane* (C_6H_{14}): 0.79; *cetane* (C_6H_{10}): 0.63; *decane* ($C_{10}H_{24}$): 0.262. Therefore, the dry oil low NO_x capability is essentially accessible to the moderate-pressure Heavy Duty GT's.

5.8. FBN-rich fuels and RQL designs

Lean premix combustion is not applicable to FBN-rich fuels as a decrease in fuel richness in the primary zone increases the conversion rate of FBN into organic NO_x. Indeed, a leaner reaction zone results in less hydrocarbon molecules competing with N· radicals for oxygen capture. On the contrary, a rich reaction zone is necessary to minimise FBN conversion. This is at the origin of the so-called rich-quench-lean, or RQL concept, where a fuel-rich combustion zone (to convert FBN in N_2) is followed by a quench and a lean zone (to minimise thermal NO_x production) [56, 57].

6. CONCLUSION: PREDICTABLE EVOLUTIONS

Within the present state-of-the-art technology of large stationary gas turbines, the most important trends as to

the evolution of energy and combustion performances can be tentatively outlined as follows.

The BACT of 25 ppm NO_x on natural gas admitted for the current dry low NO_x designs seems to coincide with the maximum firing temperature level (TRIT of 1 300–1 430 °C, [20]) afforded by the most recent progress in metallurgy, including: "directionally-solidified" and "single-crystal" buckets, "thermal barriers coating" and elaborate air cooling devices (e.g., serpentine cooling) etc. These aspects fall outside the scope of the present paper. Indeed, for the newer, highest firing temperature gas turbine generation, smoothing-out the fuel/air mixedness in the combustors is no longer a relevant solution as the NO_x emission produced by such combustion temperature levels tends to exceed 25 ppm, even in ideally premixed conditions.

There are presently diverging routes being explored as to the way of performing low NO_x combustion for this next GT generation, e.g., ultra-lean combustion resorting to active control of thermoacoustics; sequential combustion; catalytic combustion. The speed of these evolutions depends on the strength of the global environmental regulations. Emission limit values as low as 9 ppm NO_x for stationary gas turbines have already been enacted in some regions of the world and even 3 ppm in some specific urban areas, which requires resorting to SCR $DeNO_x$ or to catalytic combustion. "Dry oil low NO_x" is a further technological challenge.

Since the way to ceramic materials looks still long away for large turbine parts, it is becoming increasingly challenging to match ever more ambitious efficiency objectives requiring increasing firing temperatures. In this respect, the radical change in "cycle air management" provided by the concept of steam-cooling turbine parts looks like a very promising step ahead.

REFERENCES

[1] The world's first industrial gas turbine set at Neuchatel (1939), an international historic mechanical engineering landmark, ASME Paper, September 2, 1988.

[2] Bjorge R.W., Boericke R., O'Connor M., Kalina combined cycle power plant design and performance characteristics, in: Proceedings of the PowerGen Europe Conference (Madrid, June 1997), Penwell, Tulsa (USA), pp. 217–236.

[3] Electric Power Industrial Outlook and Atlas, Penwell Power Group, Tulsa, 1996.

[4] Brandt D.E., Wesorick R.R., Gas turbine design philosophy, in: Proceedings of the Frame 9F Congress (Paris, 1993), GEEPE Library, Belfort (France), Paper No. EGT/ 9301.

[5] Olbes A., Pujol J., Colas M., Molière M., High compatibility between gas turbines and refinery utilities, in: Proceedings of the PowerGen-Europe Conference (Madrid, June 1997), Penwell, Tulsa, pp. 453–472.

[6] Chun M.K., Song H.K., Heavy duty gas turbines in petrochemical plants, in: Proceedings of the PowerGen-Asia Conference (Singapore, September 1999) (in print).

[7] Bathie W.W., Fundamentals of Gas Turbines, 2nd edition, Wiley, London, 1996.

[8] Cohen H., Rogers G.F.C., Gas Turbine Theory, 4th edition, Wiley, London, 1996.

[9] Mathieu Ph., Nihart R., Zero emission Matiant Cycle, in: ASME IGTI & Aeroengine Congress (Stockholm, June 1998), Paper No. 98-GT-383.

[10] Aoki S., A study of hydrogen combustion turbines, ibidem, Paper No. 98-GT-384.

[11] Sawyer's Gas Turbine Engineering Handbook, 3rd edition, Vol. I: Theory and Design, Technology International Publications, Norwalk, CT, 1985.

[12] Bučko Z., Mutinski J., Gas turbines burning coal-derived fuels: the lignite gasification, power generation plant at Vresova, in: Proceedings of the PowerGen-Europe Conference (Budapest, June 1996), Penwell, Tulsa, Vol. II, pp. 316–380.

[13] Cook C.S., System evaluation and low BTU fuel combustion studies for IGCC power generation, Journal of Engineering for Gas Turbines and Power 117 (1995) 673–677.

[14] Molière M., Sire J., Heavy Duty experience with ash-forming fuels, Journal de Physique IV, Colloque C9, Supplément au Journal de Physique II 3 (1993) 719–730 (in English).

[15] Johnson R.S., The theory and operation of evaporative coolers for industrial gas turbines installations, Journal of Engineering for Gas Turbines and Power 111 (1989) 327–334.

[16] Sengschmied F., Power and economic enhancement of combined cycle power plants through inlet air cooling, in: Proceedings of the PowerGen-Asia (Delhi, 1998), Penwell, Tulsa, pp. 266–276.

[17] Jolly S., Nitzken J., Shepherd D., Evaluation of combustion turbine inlet cooling systems, ibidem, pp. 197–209.

[18] Stalder J.P., Gas turbine compressor washing: State of the art—Field experience, in: ASME IGTI & Aeroengine Congress (Stockholm, 1998), Paper No. 98-GT-420.

[19] Porte G., Turbines à gaz, Part I, ENSTA, Paris, 1987 (in French).

[20] Paul T.C., Schonewald R.W., Marolda P.J., Power systems for the 21st century: "H" gas turbine combined cycles, in: GE library, Schenectady (USA), Doc. GER 3935, 1996.

[21] Walsh P.P., Fletscher P., Gas Turbine Performance, Blackwell Science Ltd., Oxford, 1998.

[22] Dalla Betta R.A., Development of a catalytic combustor for a Heavy Duty gas turbine, in: ASME IGTI & Aeroengine Congress (Birmingham, June 1996), Paper No. 96-GT-485.

[23] Lefebvre A.W., Gas Turbine Combustion, Mac Graw Hill, New York, 1983.

[24] Mellor A.M., Design of Modern Gas Turbine Combustors, Academic Press, London, 1990.

[25] Beér J.M., Chigier N.A., Combustion Aerodynamics, 2nd ed., Robert Krieger Pub. Co, Malabar, FL, 1990.

[26] Lefebvre A.W., Atomisation and Sprays, Taylor & Francis, Bristol, PA, 1989.

[27] Bowden T.T., The influence of fuel hydrogen content upon soot formation in a model gas turbine combustor, Journal of Engineering for Gas Turbines and Power 176 (1984) 789–794.

[28] Gadiou R., Prado G., Monodimensional modelling of combustion kinetics in gas turbines, GRE scientific report dated 12/02/1996.

[29] Molière M., Becker T., Low NO_x technology for heavy duty gas turbines, in: Proceedings of "Feria de la cogeneración" (Madrid, February 1999), IFEMA, Madrid, Vol. 1, pp. 111–132.

[30] Bowman C.T., Miller J.A., Mechanism and modelling of nitrogen chemistry in combustion, Progr. Energy Combust. Sci. 15 (1989) 287–338.

[31] Bowman C.T., Control of combustion-generated NO_x emissions: Technology driven by regulation, in: 24th Symposium (Int.) Comb., The Combustion Institute, Pittsburgh, 1993, pp. 859–866.

[32] Correa S.M., A review of NO_x formation under gas turbine combustion conditions, Combust. Sci. Technol. 87 (1992) 329–362.

[33] Touchton G.L., An experimentally verified NO_x prediction algorithm incorporating the effects of steam injection, ASME Paper 84 GT 152.

[34] Becker T., Perkavec M., The capability of different semi-analytical equations for estimation of NO_x emissions of gas turbines, in: ASME Turbo Congress (The Hague, 1994), Paper No. 94 GT 282.

[35] Ruhlmann S., Molière M., Impact of FBN content on gas turbine NO_x emission, GE EPE Internal Report AGT/PBT/922-1, June 1999.

[36] Pourchot T., Analysis of performance tests of the Frame 9F gas turbine at Gennevilliers, GE EPE Internal Report, February 1993.

[37] Code of (US) Federal Regulations, Standard of Performance for Gas Turbines, USEPA, Book 40, Part 60, §60–332, 1986.

[38] Molière M., Colas M., Freimark M., Water-in-fuel emulsions to reduce the NO_x emission of gas turbines, GEC Alsthom Technical Review (Paris) 5 (1991) 47–58.

[39] Remy M., Benefits of the Frame 6B gas turbines in cogeneration plants: the UEM power plant case, Journal for Gas Turbines and Power 118 (1996) 331–336.

[40] Durilla M., Composite SCR for NO_x reduction, Engelhardt Technical Brochure, Baltimore, NJ, 1992.

[41] Rogers W., Durilla M., High temperature SCR competes with DLN combustors, Power (March 1996) 55–58.

[42] Howard J.B., Kausch W.J., Soot control by fuel additives, Progr. Energy Combust. Sci. 6 273–276.

[43] Davis L.B., Dry low NO_x combustion systems for GE heavy duty gas turbines, GE Library, Schenectady, NY, Doc. GER-3568E, 1995.

[44] Molière M., Charlesworth D., A review of European emission codes for gas turbines, in: GT Users' Panel Discussions, ASME IGTI, Stockholm, June 1998.

[45] Fric T.F., Effect of fuel unmixedness on NO_x emissions, J. Propulsion Power 9 (5) 708–713.

[46] Hiu I.Z., Correa S.M., Aerodynamics of a fuel spoke in gas turbine combustor, in: ASME IGTI Congress (Stockholm, June 1998), Paper No. 98 GT 389.

[47] Hoffman S., Further development of the Siemens LPP Hybrid burner, ibidem, Paper No. 98 GT 552.

[48] Lewis B., von Elbe G., Combustion, Flames and Explosion of Gases, 3rd edition, Academic Press, New York, 1987.

[49] Standard NFPA 325, Guide to hazard properties of flammable liquids, gases and volatile solids, NFPA, Quincy, 1994.

[50] Saeno T., NO_2 formation in the mixing region of hot burned gas with cool air—effect of surrounding air, Combust. Sci. Technol. 43 (1985) 259–269.

[51] Kiel A., The influence of burner design and turbine exhaust gas conditions on emissions of NO_x, CO and CH_4 of supplementary firing burners, Gaswaerme International 45 (1) (1996) 16–25.

[52] Morris J., Combustion aspects of application of hydrogen and natural gas fuel mixtures to MS9001E DLN-1 gas turbines at Elsta Plant, ASME IGTI (Stockholm, June 1998), Paper No. 98 GT 359.

[53] Donne P., Black S., Tziudnovsky B., Dry oil low NO_x combustion systems proven at Israel Electric Corporation, in: Proceedings of the PowerGen Europe Conference (Madrid, June 1997), Penwell, Tulsa, pp. 187–104.

[54] Van Tiggelen A., Oxydations et combustions, Editions Technip, Paris, 1968 (in French).

[55] Guibet J., Carburants et moteurs, Vol. 1, 1st edition, Editions Technip, Paris,1987 (in French).

[56] Battista R., Feitelberg A.S., Design and performance of low heating value fuel gas turbine combustors, in: ASME IGTI & Aeroengine Congress (Birmingham, June 1996), Paper No. 96 GT 531.

[57] Feitelberg A.S., Lacey M.A., The GE Rich-Quench-Lean gas turbine combustor, Journal for Gas Turbines and Power 120 (1998) 502–508.

APPENDIX I

Energy balance in a gas turbine: the various definitions of the firing temperature

In this simplified approach, we will consider a single-shaft GT running at nominal speed (e.g., 3 000 rpm) and *base load*, i.e. at the design value of the firing temperature. *Figure 1* gives the cycle schematics. For simplicity's sake, *ambient pressure* P_1 *will be kept constant* throughout this paper. It is incidentally remembered that the ISO conditions (ISO 3977) of ambient air are: 15 °C, $1.013 \cdot 10^5$ Pa and 60 % relative humidity. It is practical to take 15 °C as the origin temperature for all enthalpy data. All forms of energy losses (thermal; mechanical: power train; viscosity: pressure drops; inlet/outlet kinetic energy of fluids) are assumed independent of the fuel burnt.

Two important preliminary remarks regard the air flow and the fuel–air ratio.

(i) An axial compressor rotating at constant speed has, in its normal (T_1, P_2) operation range, a quasi-volumetric characteristic which means that the molar mass flow of the air (n_a) is proportional to the ambient air density (and stays therefore constant at constant T_1 and P_1):

$$n_{a(T_1)} = n^0_{a(T_1)} \frac{T_1^0}{T_1} \frac{P_1}{P_1^0} \tag{14}$$

or:

$$\frac{dn_a}{n_a} = -\frac{dT_1}{T_1} + \frac{dP_1}{P_1} = -\frac{dT_1}{T_1} \tag{15}$$

at constant P_1.

Note 3. – This assumes that the opening angle of the inlet guide vanes (IGV) which are devised to control to some extent the air flow into the compressor is kept constant.

(ii) Due to the high air excess that characterises GT cycles, the fuel flow represents only a small fraction of the air flow, i.e. typically $n_f/n_a \approx 0.02$–0.03 (LCV fuels are excluded).

A first complication faced when establishing the enthalpy balance of a GT comes from the air cooling flows which are bled from the compressor and used to cool various turbine hot parts (*partition vanes* or "nozzles" and rotating buckets). There are in fact different ways to define the *firing temperature* of a GT (*figure 1*):

– The first possibility is to use the combustor outlet temperature (COT): point 3″.

– Alternatively, the firing temperature can be defined upstream of the first-stage rotating buckets (point 3′) and called TRIT (turbine rotor inlet temperature). The difference between COT and TRIT simply corresponds to the cooling air stream injected into the first-stage turbine nozzles.

– However, to suppress the cumbersome flows of cooling air (n_{ar}), one can introduce the so called "ISO firing temperature" which is the fictive temperature produced at the outlet of the combustors *where all the air is assumed to pass*. This ISO firing temperature corresponds to point 3 in *figure 1c* and is denoted T_3 in this paper. Therefore: $n_{g3} \equiv n_{g4} \equiv n_g$.

Hence, the equations of energy conservation, applied to the compressor and the turbine give:

$$\begin{aligned} W_C &= n_a H_{a2} - n_a H_{a1} \\ &= n_a(H_{a2} - H_{a1}) \quad \text{(system C)} \end{aligned} \tag{16}$$

$$\begin{aligned} W_T &= n_{g3} H_{g3} - n_{g3} H_{g4} \\ &= n_{g3}(H_{g3} - H_{g4}) \quad \text{(system T)} \end{aligned} \tag{17}$$

Hence:

$$\begin{aligned} W_{GT} &= W_T - W_C \\ &= n_{g3}(H_{g3} - H_{g4}) - n_a(H_{a2} - H_{a1}) \end{aligned} \tag{18}$$

Before writing the energy balance relating to the combustors (system B), one must state two important points:

– *Hin* is defined as the product $[n_f LHV_{(T)}]$, where the subscript T specifies the reference temperature at which *LHV*, the *isothermal* combustion heat, is defined (usually $T = T_1^0 = 288$ K); therefore, *Hin* is also a function of T,

– due to the isothermal definition of *LHV*, the fuel and the air must be taken at the same initial temperature when writing the energy balance of the combustors (most likely choices are T_2 or T_8).

In order to get an expression of *Hin* containing only fuel and combustion gas data, it is judicious to mentally perform combustion at T_2 and to write that the corresponding combustion heat $Hin_{(T_2)}$ is used to heat (i) the fuel from T_8 to T_2 and (ii) the resulting combustion gas from T_2 to T_3, which gives:

$$\begin{aligned} Hin_{(T_2)} &= n_{g3}(H_{g3} - H_{g2}) \\ &\quad + n_f(H_{f2} - H_{f8}) \quad \text{(system B)} \end{aligned} \tag{19}$$

Note 4. – $Hin_{(T_1)}$ and $Hin_{(T_2)}$ are correlated by the Kirchhoff relation, a classical one in thermochemistry:

$$-\frac{dLHV_{(T)}}{dT} = \left(\sum Cp\right)_{\text{products}} - \left(\sum Cp\right)_{\text{reactants}} \tag{20}$$

The reason for the "minus" sign is to comply with the "thermodynamic convention", according to which any energy released by the system is counted negatively. This relation enables the calculation of $Hin_{(T_2)}$:

$$\begin{aligned} LHV_{(T_2)} &\approx LHV_{(T_1)} \\ &\quad - \left[\left(\sum Cp\right)_{\text{prod}} - \left(\sum Cp\right)_{\text{react}}\right](T_2 - T_1) \end{aligned}$$

and

$$\begin{aligned} Hin_{(T_2)} &\approx Hin_{(T_1)} - n_f\left[\left(\sum Cp_{12}\right)_{\text{products}}\right. \\ &\quad \left. - \left(\sum Cp_{12}\right)_{\text{reactants}}\right](T_2 - T_1) \end{aligned} \tag{21}$$

In fact, the differences between $Hin_{(T_2)}$ and $Hin_{(T_1)}$ found in applying this formula are rather low (see *table III*).

APPENDIX II

Deriving gas turbine performance data from cycle parameters

Introducing in equations (16)–(19) the notion of "average heat capacity between two points i and j", denoted Cp^{g}_{ij}, enables to write:

$$W_T = n_{g3} Cp^{g}_{34} (T_3 - T_4) \tag{22a}$$

and

$$W_C = n_a Cp^{a}_{12} (T_2 - T_1) \tag{22b}$$

so that

$$\begin{aligned} W_{GT} &= W_T - W_C \\ &= n_{g3} Cp^{g}_{34} (T_3 - T_4) - n_a Cp^{a}_{12} (T_2 - T_1) \end{aligned} \tag{23}$$

Note 5. – As T_2 undergoes limited changes (300–400 °C), Cp^{a}_{12} is assumed to be constant in this paper.

$$Hin_{(T_2)} = n_{g3} Cp^{g}_{23} (T_3 - T_2) + n_f Cp^{f}_{28} (T_2 - T_8) \tag{24}$$

Since $n_f = Hin_{(T_2)}/LHV_{(T_2)}$ and as $Cp^{f}_{82}(T_2 - T_8) \ll LHV_{(T_2)}$, one can alter equation (24) as follows:

$$Hin_{(T_2)} \approx n_g Cp^{g}_{23} (T_3 - T_2)(1 + e_{hf}) \tag{25}$$

$$\text{where } e_{hf} = Cp^{f}_{82}(T_2 - T_8)/LHV_{(T_2)} \ll 1$$

The term e_{hf} represents the fraction of the fuel energy consumed to heat the fuel from T_8 to T_2.

Finally, the GT efficiency and the enthalpy of exhaust gases are defined by:

$$\eta_{GT} = W_{GT}/Hin \tag{26}$$

$$Hex = n_{g4} Cp^{g}_{4} (T_4 - T_1) \equiv n_{g3} Cp^{g}_{4} (T_4 - T_1) \tag{27}$$

A differential approach to W_{GT}, η_{GT} and Hex is fruitful because the cycle parameters are only slightly influenced by fuel changes. To this end, it is convenient:

– to use the most common GT fuel, i.e. *methane as reference fuel*,

– to introduce as variables the ratios k_T and k_C between turbine (respectively compressor) power and overall GT power:

$$\begin{aligned} &W_T = k_T W_{GT} \quad \text{and} \\ &W_C = k_C W_{GT} \quad (\text{which implies } k_C = k_T - 1) \end{aligned} \tag{1}$$

Indeed, an analysis of the mathematic expression of k_T for a fuel f leads to the formula:

$$\begin{aligned} k_{T,f} &= k_{T,CH_4} - f(FAR_f, Cp_{g,f}, \ln \pi_f) \\ &= k_{T,CH_4} - \varepsilon(FAR_f - FAR_{CH_4}) \end{aligned}$$

in which function $\varepsilon(x)$ is a first-order infinitely small versus x. Now FAR is small and its change ($FAR_f - FAR_{CH_4}$) is still smaller. Cp_g depends little on fuel due to the large excess of N_2 and O_2 in the combustion gas. The term $\ln \pi$, as a logarithm, changes also very little in function of fuel.

The approach can be developed as follows:

$$\begin{aligned} dW_{GT} &= dW_T - dW_C = \frac{W_T\, dW_T}{W_T} - \frac{W_C\, dW_C}{W_C} \\ \frac{dW_{GT}}{W_{GT}} &= k_T \frac{dW_T}{W_T} - k_C \frac{dW_C}{W_C} \end{aligned} \tag{28}$$

where dW_T/W_T and dW_C/W_C are derived from equations (22a) and (22b),

$$\begin{aligned} \frac{d\eta_{GT}}{\eta_{GT}} &= \frac{dW_{GT}}{W_{GT}} - \frac{dHin}{Hin} \\ &= k_T \frac{dW_T}{W_T} - k_C \frac{dW_C}{W_C} - \frac{dHin}{Hin} \end{aligned} \tag{29}$$

Noting that $n_{g3} \equiv n_{g4}$, the logarithmic differentials of Hin and Hex are easy to write from equations (25) and (27):

$$\frac{dHin}{Hin} \approx \frac{dn_{g3}}{n_{g3}} + \frac{dCp^{g}_{23}}{Cp^{g}_{23}} + \frac{d(T_3 - T_2)}{T_3 - T_2} + de_{hf} \tag{30}$$

$$\frac{dHex}{Hex} = \frac{dn_{g3}}{n_{g3}} + \frac{dCp^{g}_{4}}{Cp^{g}_{4}} + \frac{d(T_4 - T_1)}{T_4 - T_1} \tag{31}$$

Using the notion of polytropic efficiency, the compression/expansion equations give:

$$T_2 = T_1 \pi^{[R/(\eta_C Cp^{a})]} \quad \text{(air compression)} \tag{32}$$

$$T_4 = T_3 \pi^{[-\eta_T R/Cp^{g}_{34}]} \quad \text{(combustion gas expansion)} \tag{33}$$

This set of equations (28)–(33) leads to expressions of dW_{GT}/W_{GT}, $d\eta_{GT}/\eta_{GT}$ and $dHex/Hex$, which are valid at constant P_1 and which express the changes in performance for small changes of the cycle conditions, like a change of fuel:

$$\begin{aligned} \frac{dW_{GT}}{W_{GT}} &= k_T \frac{dn_{g3}}{n_{g3}} + k_T \frac{dT_3}{T_3} + k_T(1-\beta)\frac{dCp^{g}_{34}}{Cp^{g}_{34}} \\ &\quad + (k_T\beta - k_C\alpha)\frac{d\ln\pi}{\ln\pi} + k_C\alpha\frac{d\eta_C}{\eta_C} + k_T\beta\frac{d\eta_T}{\eta_T} \end{aligned} \tag{34}$$

$$\frac{\mathrm{d}\eta_{GT}}{\eta_{GT}} = k_C \frac{\mathrm{d}n_{g3}}{n_{g3}} + \gamma \frac{\mathrm{d}T_1}{T_1} + (k_C - \gamma)\frac{\mathrm{d}T_3}{T_3} + (k_C - k_T\beta)\frac{\mathrm{d}Cp^g_{34}}{Cp^g_{34}} + (k_T\beta - k_C\alpha + \alpha\delta)\frac{\mathrm{d}\ln\pi}{\ln\pi} - \mathrm{d}e_{hf} + (k_C - \delta)\alpha\frac{\mathrm{d}\eta_C}{\eta_C} + k_T\beta\frac{\mathrm{d}\eta_T}{\eta_T} \quad (35)$$

$$\frac{\mathrm{d}Hex}{Hex} = \frac{\mathrm{d}n_{g3}}{n_{g3}} + \lambda\frac{\mathrm{d}T_3}{T_3} + (1-\lambda)\frac{\mathrm{d}T_1}{T_1} + (1+\mu)\frac{\mathrm{d}Cp^g_4}{Cp^g_4} - \mu\frac{\mathrm{d}\ln\pi}{\ln\pi} - \mu\frac{\mathrm{d}\eta_T}{\eta_T} \quad (36)$$

The expressions of the 6 coefficients α, β, γ, δ, λ and μ which depend only on the 4 cycle temperatures (T_1 to T_4) are given in Section 3.1 (equations (6a)–(6f)).

Note 6. – To establish equation (35), one has legitimately considered that $\mathrm{d}Cp^g_{34}/Cp^g_{34} \approx \mathrm{d}Cp^g_{23}/Cp^g_{23}$.

Note 7. – The term $-\mathrm{d}e_{hf}$ must not be omitted in the expression of $\mathrm{d}\eta_{GT}/\eta_{GT}$ (equation (35)). For instance, $e_{hf,CH_4} = 1.85\,\%$ and $e_{hf(H_2)} = 4\,\%$, so that, when passing from CH_4 to H_2, the differential $\mathrm{d}e_{hf}$ equals $-2.15\,\%$.

Case of an ideal closed Brayton cycle (ICBC)

In an ICBC, where namely combustors are replaced by heat exchangers (no fuel added), one has

$$T_3 \equiv T_3', \quad \eta_C = \eta_T = 1, \quad k_C = \frac{T_2}{T_3 - T_2}, \quad k_T = \frac{T_3}{T_3 - T_2}, \quad n_{g3} \equiv n_a, \quad Cp^g \equiv Cp^a$$

so that:

$$W_{GT} = n_a Cp^a\left\{T_3\left[1 - \pi^{(-R/Cp^a)}\right] - T_2\left[1 - \pi^{(-R/Cp^a)}\right]\right\} = n_a Cp^a(T_3 - T_2)\left[1 - \pi^{(-R/Cp^a)}\right] \quad (37)$$

$$Hin = n_a Cp^a(T_3 - T_2) \quad \text{and} \quad \eta_{GT} = \left[1 - \pi^{(-R/Cp^a)}\right] \quad (38)$$

Note 8. – Assimilating air to a diatomic perfect gas, moreover, yields $R/Cp^a = 2/7$ and $\eta_{GT} = (1 - \pi^{-0.287})$ = const. So, in an ICBC gas turbine, the performances would obey the following trends:

– efficiency would be independent of T_3 but would just increase with π,

– power would increase with π as well and be a linearly increasing function of T_3 and $(-T_1)$.

APPENDIX III

Deriving $\mathrm{d}W_{GT}/W_{GT}$, $\mathrm{d}\eta_{GT}/\eta_{GT}$ and $\mathrm{d}Hex/Hex$ from fuel properties

In order to assess in a straightforward way the influence of fuel on performances, one must express in equations (34)–(36) the differentials $\mathrm{d}n_g/n_g$ and $\mathrm{d}Cp^g/Cp^g$ in function of fuel properties. To that end, let us take $C_cH_hN_nS_sO_o$ as general molecular formula of the fuel. This "fictive" formula rarely represents a pure chemical but generally designates a mixture which may include some inerts (but no FBN). For instance: $CH_4 + H_2 + N_2$ would be noted $C_1H_6N_2$.

Let φ_3 be the "ISO-richness" in the combustors: by analogy with the definition of T_3, "ISO" means that the combustors are assumed to receive the whole compressor air flow plus the actual fuel flow. φ_3 is not the true combustion richness but the concentrations of CO_2, SO_2 and H_2O deduced from φ_3 are identical to those at point 4.

Using φ_3, the combustion reaction may be written:

$$\varphi_3 C_cH_hN_nS_sO_o + \omega(O_2 + \nu N_2) \rightarrow \varphi_3 cCO_2 + \varphi_3 sSO_2 + \varphi_3\frac{h}{2}H_2O + \varphi_3\frac{n}{2}N_2 + (1-\varphi_3)\omega O_2 + \omega\nu N_2$$

where $(O_2 + \nu N_2)$ is a formula for air (with $\nu \approx 3.76$) and $\omega = (c + h/4 + s - o/2)$.

Remembering that $n_f = Hin/LHV$, the fuel richness φ_3 can be written:

$$\varphi_3 = \omega(1+\nu)\frac{n_f}{n_a} = \frac{Hin\omega(1+\nu)}{n_a LHV} \quad (39)$$

From the above combustion equation, one can deduce the following expression of the molar combustion gas flow n_{g3}:

$$n_{g3} = n_a + q_f n_f = n_a\left(1 + \frac{q_f n_f}{n_a}\right) \quad (40)$$

where $q_f = h/4 + o/2 + n/2$. Let us define *SGF*, the specific (combustion) gas flow, as

$$SGF = n_{g3}/n_a \quad (41)$$

If one defines the specific heat input *SHI* as $SHI = Hin/n_a$, one can write, since $n_f = Hin/LHV$:

$$SGF = 1 + q_f FAR = 1 + \frac{q_f n_f}{n_a} = 1 + q_f\frac{Hin/n_a}{LHV} = 1 + q_f\frac{SHI}{LHV} \quad (2)$$

and, according to equations (2′) and (15):

$$\frac{\mathrm{d}n_{g3}}{n_{g3}} = \frac{\mathrm{d}n_a}{n_a} + \frac{\mathrm{d}SGF}{SGF} = -\frac{\mathrm{d}T_1}{T_1} + \mathrm{d}(q_f FAR) \qquad (42)$$

Substituting this expression of $\mathrm{d}n_g/n_g$ in equations (34)–(36) yields the expressions of $\mathrm{d}W_{GT}/W_{GT}$, $\mathrm{d}\eta_{GT}/\eta_{GT}$ and $\mathrm{d}Hex/Hex$ which are given in equations (3)–(5) and are extensively exploited in Section 3.

APPENDIX IV

Thermal NO_x index versus stoichiometric combustion temperature Tc_s

Since the residence time τ_B in a GT flame is short and the kinetics of thermal NO_x is, according to Arrhenius' equation, an exponential function of the combustion temperature, one can write:

$$[\mathrm{NO}] \approx \left\{\frac{\mathrm{d}[\mathrm{NO}]}{\mathrm{d}t}\right\}_{rz} \tau_B \propto P_2^m \exp\left[-E^{\neq}/(RTc_s)\right]\tau_B \qquad (43)$$

where Tc_s is the *adiabatic stoichiometric combustion temperature* (taking account of molecular dissociations) and $E^{\neq}$ is the activation energy of Zeldovich'es mechanism limiting step ($E^{\neq}$ is independent of the fuel nature).

Due to the high air excess that characterises combustion in GT, τ_B which is the ratio between the volume flow of the reacting air/fuel mixture and the liner volume, is virtually independent of the fuel nature (for a common range of fuels, excluding LCV fuels). So, noting $T^{\neq}$ the term $E^{\neq}/R$:

$$[\mathrm{NO}] \approx \mathrm{const} \cdot P_2^m \exp\left[-T^{\neq}/Tc_s\right] \qquad (44)$$

Moreover, as Tc_s is usually comprised between 2 200 and 2 500 K, the ratio between the NO_x emissions of two fuels can be written using a first-order expansion of $1/Tc_s$:

$$\frac{\mathrm{NO}_{x_2}}{\mathrm{NO}_{x_1}} = \exp\left[-T^{\neq}\left(\frac{1}{Tc_{s2}} - \frac{1}{Tc_{s1}}\right)\right] \approx \exp\left[\frac{(Tc_{s2} - Tc_{s1})T^{\neq}}{2\,350^2}\right]$$

Thus, at constant operational and ambient conditions and for a given combustion design/geometry, the NO_x emission data of a series of fuels obeys, in a first-approach, an exponential law:

$$\mathrm{NO}_x = K P_2^m \exp\left[k' Tc_s\right] \qquad (45)$$

where $k' = E^{\neq}/(2\,350^2 R)$. Now, in the *stoichiometric conditions*, denoted by the letter s, the combustion reaction can be written:

$$\mathrm{C}_c\mathrm{H}_h\mathrm{S}_s\mathrm{O}_o\mathrm{N}_n + \omega(\mathrm{O}_2 + \nu\mathrm{N}_2) \rightarrow c\mathrm{CO}_2 + s\mathrm{SO}_2 + \frac{h}{2}\mathrm{H}_2\mathrm{O} + \left(\nu\omega + \frac{n}{2}\right)\mathrm{N}_2 \qquad (46)$$

where $\omega = c + h/4 + s - o/2$ as above.

Like in Appendix III, the formula $\mathrm{C}_c\mathrm{H}_h\mathrm{S}_s\mathrm{N}_n\mathrm{O}_o$ may include inert gases (H_2O, N_2 and CO_2 etc.).

Since enthalpy data at 15 °C is taken equal to zero for all species, the energy balance between point 2 and point s allows to write, assuming that the fuel temperature at injection port (T_8) is 288 K:

$$H_{g(Tc_s)} \equiv c\,H_{CO_2(Tc_s)} + \frac{h}{2}H_{H_2O(Tc_s)} + s\,H_{SO_2(Tc_s)} + \left(\nu\omega + \frac{n}{2}\right)H_{N_2(Tc_s)} = LHV_{(T_1)} + \omega H_{a2} - E^{dis} \qquad (47)$$

E^{dis} is the energy of dissociation of the reaction products in the flame front, an endothermal process which leads to the formation of O_2, CO and radicals like H, OH, O and is enhanced at increasing flame temperature (molecular dissociations tend thus to oppose any Tc_s rise).

The various enthalpic terms $H_{i(Tc_s)}$ of the left-hand side of equation (47) are polynomial functions of the temperature but, because Tc_s usually varies between 2 200 and 2 500 K, one can write, for each species i:

$$H_{i(Tc_s)} \approx \check{C}p^i \cdot \left(Tc_s - T_1^0\right), \qquad (48)$$

where $\check{C}p^i$ is the averaged molar heat capacity of species i between T_1^0 (15 °C) and 2 350 K. Hence:

$$Tc_s - T_1^0 \approx \frac{LHV + \omega H_{a(T_2)} - E^{dis}}{\check{C}p^g} = \frac{LHV + \omega H_{a(T_2)} - E^{dis}}{c\check{C}p^{CO_2} + \frac{h}{2}\check{C}p^{H_2O} + \check{C}p^{SO_2}_{(Tc_s)} + \left(\nu\omega + \frac{n}{2}\right)\check{C}p^{N_2}} \qquad (49)$$

Combining (45) and (49) and taking, for simplicty's sake, a fuel exempt of sulphur:

$$\mathrm{NO}_x = k P_2^m \exp\left[k' Tc_s\right] = k P_2^m \exp\left[\frac{k'(LHV + \omega H_{a2} - E^{dis})}{c\check{C}p^{CO_2} + \frac{h}{2}\check{C}p^{H_2O} + \left(\nu\omega + \frac{n}{2}\right)\check{C}p^{N_2}}\right] \qquad (9)$$

This formula is thoroughly analysed in Section 5.

APPENDIX V

NO_x emission data for "mixture combustion"

"Mixture combustion" means that two distinct fuels are burnt simultaneously in a same GT. Let x_j be the molar proportion of fuel j in the mixture ($x_j = n_{\text{fuel}\,j}/[n_{\text{fuel}\,1} + n_{\text{fuel}\,2}]$). For the separate combustion of each fuel j, the combustion equation writes:

$$\mathrm{C}_{c_j}\mathrm{H}_{h_j}\mathrm{S}_{s_j}\mathrm{O}_{o_j}\mathrm{N}_{n_j} + \omega_j(\mathrm{O}_2 + \nu\mathrm{N}_2) \rightarrow c_j\mathrm{CO}_2 + s_j\mathrm{SO}_2 + \frac{h_j}{2}\mathrm{H}_2\mathrm{O} + \left(\nu\omega_j + \frac{n_j}{2}\right)\mathrm{N}_2$$

where $\omega_j = c_j + h_j/4 + s_j - o_j/2$. Neglecting the E^{dis} term, equations (47) and (48) yield, for each fuel:

$$\check{C}p^{\text{g}}_{(\text{fuel}\,1)}\left(Tc_{\text{s}(1)} - T_1^0\right) = LHV_{(1)} + \omega_1 H_{\text{a}(T_2)} \quad (50\text{a})$$

$$\check{C}p^{\text{g}}_{(\text{fuel}\,2)}\left(Tc_{\text{s}(2)} - T_1^0\right) = LHV_{(2)} + \omega_2 H_{\text{a}(T_2)} \quad (50\text{b})$$

where $\check{C}p^{\text{g}}_{(\text{fuel}\,j)}$ is the heat capacity of the combustion gas generated by fuel j, averaged between 288 and 2 350 K.

Let us take $c_j = 1$. Due to the large excess of air in GT's and the high concentrations of N_2 and O_2 in the combustion gas, one can assume, for usual fuels (it is virtually the case for all hydrocarbons), that

$$\check{C}p^{\text{g}}_{(\text{fuel}\,1)} \approx \check{C}p^{\text{g}}_{(\text{fuel}\,2)} = \check{C}p^{\text{g}}_{\text{mixture}}$$

Since $x_1\omega_1 + x_2\omega_2 \equiv \omega_{(\text{mixture})}$ and $LHV_{(\text{mixture})} \equiv x_1 LHV_{(1)} + x_2 LHV_{(2)}$, one can multiply equations (50a) and (50b) by x_1 and x_2, respectively, and sum them, which gives:

$$\check{C}p^{\text{g}}_{(\text{mixture})}\left(x_1 Tc_{\text{s}(1)} + x_2 Tc_{\text{s}(2)} - T_1^0\right) = LHV_{(\text{mixture})} + \omega_{(\text{mixture})} H_{\text{a}(T_2)}$$

The form of this equation, identical to that of (50a) and (50b), means that:

$$Tc_{\text{s}(\text{mixture})} = x_1 Tc_{\text{s}(1)} + x_2 Tc_{\text{s}(2)} \quad (51)$$

Therefore, equation (45) gives the geometric law alluded in Section 5.1.3:

$$\mathrm{NO}_{x\,(\text{mixture})} = (\mathrm{NO}_{x\,\text{fuel}\,1})^{x_1}(\mathrm{NO}_{x\,\text{fuel}\,2})^{x_2} \quad (19)$$

This amazingly simple formula results from the linearity of equation (51).

APPENDIX VI

Effect of diluent injection on energy and emission performances

Let d be the symbol for the diluent being injected and 9 the label of the diluent injection point (*figure 1*).

A. Effect on NO_x emission

In the case of steam or water injection, the reaction in the stoichiometric zone is:

$$\mathrm{C}_c\mathrm{H}_h\mathrm{O}_o\mathrm{N}_n + \omega(\mathrm{O}_2 + \nu\mathrm{N}_2) + RI_{\text{rz}}\mathrm{H}_2\mathrm{O} \rightarrow c\mathrm{CO}_2 + \left(\frac{h}{2} + RI_{\text{rz}}\right)\mathrm{H}_2\mathrm{O} + \left(\nu\omega + \frac{n}{2}\right)\mathrm{N}_2 \quad (52)$$

where RI_{rz} is the injection rate of H_2O in the reaction zone, ie the ratio between the number of H_2O molecules reaching the reaction zone and the number of fuel molecules in the same.

To obtain Tc_{s}, one must add, in the flame front enthalpy balance, the sensible heat of the diluent ($H_{\text{d}9}$) and eventually its latent heat of vaporization (Lv_{d}). The exponential law (9) giving the NO_x emission becomes, for any diluent d:

$$\begin{aligned}\mathrm{NO}_{x_{RI}} &= k P_2^m \exp[k_2 Tc_{\text{s}}] \\ &= k P_2^m \exp\Big\{\big[k' LHV_{(T_1)} + \omega H_{\text{a}(T_2)} - E^{\text{dis}}_{(RI)} \\ &\quad - RI_{\text{rz}}(Lv_{\text{d}} - H_{\text{d}9})\big] \\ &\quad \cdot \left[c\check{C}p^{\mathrm{CO}_2} + \frac{h}{2}\check{C}p^{\mathrm{H}_2\mathrm{O}} + \left(\nu\omega + \frac{n}{2}\right)\check{C}p^{\mathrm{N}_2} + RI_{\text{rz}}\check{C}p^{\text{d}}\right]^{-1}\Big\}\end{aligned} \quad (53)$$

Note 9. – In this equation $E^{\text{dis}}_{(RI)}$ is a decreasing exponential function of RI. Indeed, the higher RI, the lower Tc_{s}, the lower the dissociation rates: $E^{\text{dis}}_{(RI)} = E^{\text{dis}}_{(RI=0)}\exp(-\sigma RI)$. For instance, for methane combustion and steam injection, one has $\sigma \approx 0.49$. However, because the mole fractions of dissociated molecules are in the range of 10^{-3}–10^{-5}, $E^{\text{dis}}_{(RI)}$ is much smaller than $H_{\text{a}(T_2)}$ and can be neglected in practice.

Since the terms associated with RI in equation (53) are small, a first-order expansion with respect to RI gives:

$$\ln(\mathrm{NO}_{x_{RI}}) - \ln(\mathrm{NO}_{x_{RI=0}}) = -RI_{\text{rz}}\left[\frac{Lv_{\text{d}} - H_{\text{d}9}}{A} + \frac{\check{C}p^{\text{d}}}{B}\right]\ln(\mathrm{NO}_{x_{RI=0}}) \quad (54)$$

where parameters A and B are independent of the injection rate RI but depend on: (i) T_2 (so on π); (ii) fuel composition, LHV and coefficients of stoichiometric combustion:

$$A = (LHV_{(T_1)} + \omega H_{a(T_2)}) \quad \text{and}$$
$$B = c\check{C}p^{CO_2} + \frac{h}{2}\check{C}p^{H_2O} + \left(\nu\omega + \frac{n}{2}\right)\check{C}p^{N_2} \tag{55}$$

Experience shows that for the usual values of RI, a linear expansion can also bee used:

$$(NO_{x_{RI}}) = (NO_{x_{RI=0}})\left\{1 - RI_{rz}\ln(NO_{x_{RI=0}}) \cdot \left[\frac{Lv_d - H_{d9}}{A} + \frac{\check{C}p^d}{B}\right]\right\} \tag{12}$$

B. Effect on energy performances

All operation conditions are assumed constant except those relating to the injection of diluent. Moreover, turbine and compressor polytropic efficiency data are assumed unchanged by diluent injection. In equations (3) and (4), the variation of the parameter $q_f FAR$ associated with the diluent injection can be simply written by incorporating the diluent into the fuel composition ($C_cH_hS_sO_oN_n$) whatever the injection mode ($DeNO_x$ or power augmentation):

$$C_cH_hS_sO_oN_n + RI_9H_2O \Leftrightarrow C_cH_{(h+2RI_9)}S_sO_{(o+RI_9)}N_n$$

This formula becoming the new molecular formula of the fuel, equation (2) gives (the change in FAR is very small):

$$\Delta(q_f FAR) \approx FAR\left[\left(\frac{h}{4} + \frac{RI_9}{2} + \frac{o}{2} + \frac{RI_9}{2} + \frac{n}{2}\right) - \left(\frac{h}{4} + \frac{o}{2} + \frac{n}{2}\right)\right] = FAR\,RI_9 > 0 \tag{56}$$

One can easily show that the change in Cp^g resulting from a water or steam injection can be written:

$$\frac{\Delta Cp^g}{Cp^g} \approx RI_9 FAR'\left(\frac{Cp^d}{Cp^g_{(RI=0)}} - 1\right) \tag{57}$$

where $FAR' = FAR(1 - q_f FAR)$.

B1. Change in power output. Besides ($q_f FAR$), the sole other term altered in equation (3) is Cp^g. For water or steam injection, $\Delta Cp^g/Cp^g$ is positive as Cp^{H_2O} is higher than both Cp^{N_2} and Cp^{O_2}. The change in $(\ln\pi)$ is minute and can be neglected. Equation (3) leads to:

$$\frac{\Delta W_{GT}}{W_{GT}} = k_T\Delta(q_f FAR) + k_T(1-\beta)\frac{\Delta Cp^g_{34}}{Cp^g_{34}} = k_T RI_9 FAR\left[1 + (1-\beta)\left(\frac{Cp^d_{34}}{Cp^g_{34(RI=0)}} - 1\right) \cdot (1 - q_f FAR)\right]$$

Remembering the definition of k_T, one obtains the following relation showing a linear dependence of ΔW_{GT} upon RI_9:

$$\Delta W_{GT} = W_T RI_9 FAR\left[1 + (1-\beta)\left(\frac{Cp^d_{34}}{Cp^g_{34(RI=0)}} - 1\right) \cdot (1 - q_f FAR)\right] = W_T RI_9 FAR\,\psi\left(\beta, \frac{Cp^d}{Cp^g}, FAR\right) \tag{58}$$

where:

– $(1-\beta)$ is always positive ($\beta = 0.771$ in the example of Section 3.2),

– $(Cp^d_{34}/Cp^g_{34(RI=0)} - 1)$ is positive for $d = H_2O$ or CO_2 and negative for $d = N_2$ or a rare gas.

But the function $\psi(\beta, Cp^d/Cp^g, FAR)$ is always positive so that any diluent injection always increases W_{GT}, which is a physical necessity.

B2. Change in efficiency. In equation (4) giving $d\eta_{GT}$, the enthalpy balance (25) of the combustion chambers must be altered as follows:

$$Hin_{(T_2)} = n_{g3}Cp^g_{23}(T_3 - T_2) + n_f Cp^f_{28}(T_2 - T_8) + (n_f RI_9)Cp^d_{29}(T_2 - T_9) + (n_f RI_9)Lv_{d(T_2)} \tag{25b}$$

The latent heat $Lv_{d(T_2)}$ is zero if the diluent is gaseous and must be taken at temperature T_2 for the same reasons as in Appendix II. Substituting the expression of $n_f = Hin_{(T_2)}/LHV_{(T_2)}$ further gives:

$$Hin_{(T_2)} = n_{g3}Cp^g_{23}(T_3 - T_2)(1 + e_{hf} + e_{shd} + e_{lhd}) \tag{59}$$

where

$$e_{hf} = \frac{Cp^f_{28}(T_2 - T_8)}{LHV}$$
$$e_{shd} = \frac{RI_9 Cp^d_{29}(T_2 - T_9)}{LHV}$$

and

$$e_{lhd} = \frac{RI_9 Lv_{d(T_2)}}{LHV}$$

The subscripts “shd” and “lhd” are respectively for “sensible heat of diluent” and “latent heat of diluent”.

Then the change in heat input caused by diluent injection (equation (35)) can be written:

$$\frac{\Delta Hin}{Hin} = \frac{\Delta n_{g3}}{n_{g3}} + \frac{\Delta Cp^{g}_{23}}{Cp^{g}_{23}} + \frac{\Delta(T_3 - T_2)}{T_3 - T_2} + \Delta e_{hf} + \Delta e_{shd} + \Delta e_{lhd}$$

This leads to the following expression of the change in efficiency associated with diluent injection:

$$\frac{\Delta\eta_{GT}}{\eta_{GT}} = k_C \Delta(q_f FAR) + (k_C - k_T\beta)\frac{\Delta Cp^{g}_{34}}{Cp^{g}_{34}} + (k_T\beta - k_C\alpha + \alpha\delta)\frac{\Delta \ln \pi}{\ln \pi} - \Delta e_{hfd} \quad (4')$$

where e_{hfd} (energy consumed to heat fuel and diluent) equals:

$$\Delta e_{hfd} = \Delta e_{hf} + \Delta e_{shd} + \Delta e_{lhd} \approx \Delta e_{shd} + \Delta e_{lhd} = RI_9 \frac{Cp^{d}_{29}(T_2 - T_9) + Lv_{d(T_2)}}{LHV}$$

A further processing of this expression using equation (57) leads to the following approximate for $\Delta\eta_{GT}/\eta_{GT}$:

$$\frac{\Delta\eta_{GT}}{\eta_{GT}} \approx RI_9 \left\{ k_C FAR + (k_C - k_T\beta) \cdot FAR' \left(Cp^{d}_{34} - Cp^{g}_{34(RI=0)}\right) - \frac{Cp^{d}_{28}(T_2 - T_8)}{LHV} - \frac{Lv_{d(T_2)}}{LHV} \right\} \quad (60)$$

where $FAR' = FAR(1 - q_f FAR)$.

One can see that, in the case of steam injection ($Lv_{d(T_2)} = 0$), efficiency increases since the sole negative term is minute compared with the two first terms. In contrast, in the case of liquid water injection, efficiency declines due to the high value of the negative term containing Lv_d.

Both the relative changes in W_{GT} and η_{GT} are approximately proportional to the diluent injection rate RI_9.